cortical plate, with limited expression in ventricular zone progenitors (Shimizu *et al.* 1995). Although this group is thought to regulate later events in neuronal differentiation during development, their persistent expression in the adult nervous system suggests a role in promoting and maintaining gene expression in mature neurons.

Math2, a structural homolog of the product of the *Drosophila* proneural gene *atonal*, was molecularly isolated and characterized in mouse brain (Bartholoma and Nave 1994). It is expressed exclusively and abundantly in the CNS. Functional studies showed that Math2 is involved in neurite regeneration and neuronal survival in PC12 cells (Uittenbogaard and Chiaramello 2002, 2005). Math2-positive progenitor cells are generated by ventricular zone cells, which in turn migrate into the subventricular zone and then differentiate into glutamatergic neurons in the upper cortical layers (Wu *et al.* 2005). *In situ* hybridization analysis has demonstrated high levels of Math2 mRNA in mature pyramidal neurons of the hippocampus, cerebellum, and several neocortical areas previously associated with learning and memory formation (Bartholoma and Nave 1994). This suggests that Math2 plays a potential role in synaptic plasticity and maintenance of differentiated neurons (Bartholoma and Nave 1994).

We have previously performed expressed sequence tag analysis (Yamada *et al.* 1999, 2000) and found that chronic antidepressant treatment up-regulates Math2 gene expression in rat frontal cortex. To clarify the role of Math2, in this study, we investigated the target genes regulated by Math2 in cultured rat cortical cells. Transcriptional regulation of target genes was assessed by chromatin immunoprecipitation (ChIP) assay and luciferase assay. In addition, neuronal function mediated by the Math2-target gene cascade was also investigated in PC12 cells.

Experimental procedures

Cell cultures

Cerebral cortices from 19-day-old fetal rats (E19) (Clea Japan, Tokyo, Japan) were dissected in a Ca^{2+}-free Hank's solution (pH 7.4; Sigma Chemical, St Louis, MO, USA). Tissues were washed with Ca^{2+}-free Hank's solution and then treated with 0.25% trypsin (Invitrogen, San Diego, CA, USA) and 0.1% Dnase (Sigma Chemical) for 30 min at 37°C. Trypsin digestion was terminated by adding culture medium containing 0.1% Dnase, and tissues were triturated with a pipette. The culture medium used was Eagle's minimum essential medium (Sigma Chemical) supplemented with 10% fetal calf serum; 5% glucose (Wako, Osaka, Japan); 2 mM L-glutamine (Invitrogen); and 0.02 mg/mL gentamycin (Invitrogen). Dispersed cells were collected by centrifugation at 900 *g* for 5 min at 4°C, resuspended in culture medium, and passed through a cell strainer (mesh size, 70 μm; BD Falcon, Franklin Lakes, NJ, USA). The cells were then plated at a final density of $4 \times 10^5/cm^2$ on poly-L-lysine-coated 10-cm dishes (Iwaki, Tokyo, Japan) and cultured at 37°C in a humidified atmosphere containing 5% CO_2. This study was carried out in accordance with the *Guide for the Care and Use of Laboratory Animals* of the National Center of Neurology and Psychiatry, which is accredited by the Ministry of Education, Culture, Sport, Science, and Technology, Japan.

PC12 cells were cultured in Dulbecco's modified Eagle's medium (Sigma Chemical) supplemented with 10% fetal calf serum, 5% horse serum (Invitrogen), 100 U/mL penicillin, and 100 μg/mL streptomycin (Invitrogen) at 37°C in a humidified atmosphere containing 5% CO_2. The medium was replaced with culture medium twice a week.

Sample preparation for GeneChip® analysis

Rat Math2 cDNA was amplified by PCR and cloned into the *SalI*/*XhoI* site of a pCMV-Myc vector (Takara, Shiga, Japan). Using TransFectin transfection reagent (BioRad, Hercules, CA, USA), we co-transfected cortical cells cultured in a 10-cm dish with 13.3 μg of Math2 expression vector or control vector and 2.7 μg of low-affinity nerve growth factor receptor (LNGFR) expression vector (Miltenyi Biotec, Bergisch Gladbach, Germany) that encoded a cytoplasmically truncated cell surface marker. After incubation for 24 h, the cells were separated with a MACSelect LNGFR Transfected Cell Selection Kit (Miltenyi Biotec) according to the manufacturer's protocol. Briefly, cells were washed with phosphate-buffered saline (PBS) and then treated with 0.25% trypsin (Invitrogen) for 2 min. Trypsin digestion was terminated by adding fetal calf serum. The cells were incubated with monoclonal anti-LNGFR-coupled paramagnetic microbeads for 15 min at 4°C, and then separated in columns subjected to a magnetic field.

GeneChip® analysis

After separation of the transfected cultured cortical cells, total RNA was extracted with Isogen reagent (Nippon Gene Co., Tokyo, Japan). Micorarray analysis was performed according to the manufacturer's protocol (Affymetrix, Santa Clara, CA, USA). Briefly, 50 ng of total RNA was used for cDNA synthesis with a Two-Cycle Target Labeling Kit (Affymetrix). Biotinylated cRNA was fragmented, and 15 μg of the fragmented cRNA was hybridized to a GeneChip® Rat Genome 230 2.0 array (Affymetrix), which contains probes for 31 100 genes. The quality of total RNA and cRNA was analyzed with a BioAnalyzer (Agilent Technologies Inc., Santa Clara, CA, USA). Each sample from an individual dish of cultured cortical cells was hybridized to an array. The samples were hybridized for 16 h at 45°C under constant rotation (60 rpm) in a GeneChip® Hybridization Oven 640 (Affymetrix). After hybridization, microarrays were washed, stained with streptavidin phycoerythrin in a GeneChip® Fluidics Station 450 (Affymetrix), and scanned with a GeneChip® Scanner 3000 (Affymetrix).

Data analysis

The raw microarray data were processed with Affymetrix MicroArray Suite software, version 5.0 (Hubbell *et al.* 2002). To normalize the probe intensity across different chips, the top 2% and bottom 2% of signal intensities were excluded, and then the mean were calculated. The data were then imported into GeneSpring 7.2 software (Silicon-Genetics, Redwood, CA, USA). For the functional clustering analysis, the resulting 46 genes were analyzed using The Database for Annotation, Visualization, and Integrated Discovery (DAVID 2.0; released 11/2007; http://www.david.abcc.ncifcrf.gov/home.jsp) based on gene ontology (GO)

© 2008 The Authors
Journal Compilation © 2008 International Society for Neurochemistry,

annotations (Dennis *et al.* 2003). The Fisher's Exact test was applied to evaluate the statistical significance of the association between the 46 genes and GO database ($p < 0.05$). GO terms were described according to the GO database (http://www.geneontology.org/).

Samples for real-time quantitative PCR

Cultured rat cortical cells and PC12 cells transfected with Math2 expression vector or control vector were used for real-time RT-PCR.

In the cultured cortical cell experiments, we used cDNA prepared for GeneChip analysis. PC12 cells (1×10^6 cells) were seeded onto poly-L-lysine-coated 6-cm diameter dishes, transfected with 5 μg of Math2 expression vector or control vector using 15 μL TransFectin reagent (BioRad), and cultured for 24 h. Total RNA was extracted, and cDNA was synthesized using oligo (dT) primers and Super-Script III reverse transcriptase (Invitrogen).

Real-time quantitative PCR

Real-time quantitative PCR was used to quantify Math2 and plasticity-related gene 1 (Prg1) mRNA expression in cultured cortical cells and PC12 cells using an ABI PRISM 7000 instrument (Applied Biosystems, Foster City, CA, USA). PCR primers were designed with Primer Express Software (Applied Biosystems). The primers used for rat Prg1 were 5′-CAGGTGGTATCTCTTCTTAG TGTTCTATTT-3′ and 5′-CTCTTTATTCAATACTCGGTTTCAT CA-3′ (Invitrogen). The primer pair for β-actin, which was used as a reference for gene amplification, was 5′-TCGCTGACAG GATGCAGAAGG-3′ and 5′-GCCAGGATAGAGCCACCAAT-3′ (Invitrogen). The SYBR® Green PCR Core Reagents Kit (Applied Biosystems) was utilized for fluorescence detection of cDNA. For quantification, we used the standard curve method (User Bulletin, ABI PRISM 7000 Sequence Detection System). Briefly, for rat Prg1 and β-actin, an absolute standard curve was obtained by plotting the threshold cycle following PCR amplification of serial dilutions of the control cDNA template. Data were given as percentages of the control value (mean ± SEM).

The statistical significance of differences between controls and Math2 transfectants in cultured cortical cells and PC12 cells was analyzed with Student's t-tests. Tukey–Kramer was used to analyze data from the Prg1-siRNA study. A value of $p < 0.05$ was regarded as significant.

Chromatin immunoprecipitation assay

PC12 cells (5×10^6 cells) were seeded onto poly-L-lysine-coated 10-cm diameter dishes, transfected with 16 μg of Math2 expression vector or control vector using 40 μL TransFectin reagent (BioRad), and cultured for 24 h. Cells were cross-linked with 1% formaldehyde in Dulbecco's modified Eagle's medium for 10 min at 25°C. The cross-linking reaction was quenched by adding 125 mM glycine. The cells were then washed in ice-cold PBS and incubated for 20 min on ice in lysis buffer containing 50 mM Tris, pH 8.0, 10 mM EDTA, 1% sodium dodecyl sulfate (SDS), and 0.4 mM Pefabloc SC peptidase inhibitor (Roche, Mannheim, Germany). Lysates were sonicated with an Ultrasonic disruptor (UD-200; Tomy, Tokyo, Japan) at power 5. The vast majority of chromatin fragments generated were under 500 bp (results not shown). The fragmented DNA was then centrifuged at 12 000 *g* for 10 min at 4°C, and the supernatant was collected. Dilution buffer containing 10 mM Tris, pH 8.0, 300 mM NaCl, 5 mM EDTA, and 0.5% SDS was added, and 1/10 volume of the diluent was stored as input for the positive control. The samples were pre-cleaned with Protein G sepharose with rotation for 1 h at 4°C. After centrifugation, 6 μg of anti-Myc antibody (Invitrogen) or mouse IgG antisera (Santa Cruz Biotechnology, Santa Cruz, CA, USA) was added to the supernatant, and immune complexes were allowed to form overnight at 4°C. Protein G sepharose was then added, and the mixture was incubated for an additional 2 h at 4°C. The immune-protein G sepharose complexes were washed five times in wash buffer (50 mM Tris, pH 8.0, 150 mM NaCl, 1 mM EDTA, 1% SDS, and 0.1% sodium deoxycholate), and the DNA was eluted with elution buffer (10 mM Tris, pH 8.0, 300 mM NaCl, 5 mM EDTA, and 0.5% SDS). Cross-links were reversed by incubating the DNA overnight at 65°C. The samples were digested with 30 μg/mL Rnase A and 75 μg/mL proteinase K for 1 h at 55°C. The DNA was purified and dissolved, and then the samples and a 1 : 10 dilution of the purified input chromatin were subjected to 35 PCR cycles (denaturation at 94°C, annealing at 55°C, and extension at 72°C) using TaqEX DNA polymerase (Takara). The products were visualized by electrophoresis on 2% agarose gels (Invitrogen) containing ethidium bromide. PCR primers were designed to amplify the three sets of primers for the Prg1 promoter (primer set A: 5′-$^{-519}$CACGATTTACCTGGGGTAGA^{-500}-3′ and 5′-$^{-360}$GG CCCTATTCATAACATTCGTG^{-381}-3′; primer set B: 5′-$^{-395}$CA CAGGTAGTGAGACACGAA^{-376}-3′ and 5′-$^{-183}$TCTACAGCA GAAACACGCAA^{-202}-3′; primer set C: 5′-$^{-177}$ACAGTAA TGGTTGCCAAGAG^{-158}-3′ and 5′-$^{-15}$AGCTCAGGAAATG TTCTAACC^{-35}-3′) and a set of primers for the coding region (primer set D: 5′-$^{+265}$TGCTCTCTAGAAAGGCAAC^{+283}-3′ and 5′-$^{+492}$GGAAAGTGATAGCCAGCT^{+475}-3′).

Promoter assay

We constructed a series of 5′-end deletion mutants of the Prg1 promoter region, amplified them by PCR, and cloned them into the *Eco*RV/*Bgl*II site of a promoter-less reporter plasmid, pGL4.10 firefly luciferase vector (Promega, Madison, WI, USA). We co-transfected human embryonic kidney (HEK293) cells cultured in 12-well plates (3×10^5 cells per well) with 1.65 μg DNA containing 0.8 μg reporter plasmid, 0.8 μg Math2 expression vector or control vector, and 0.05 μg reference plasmid [pGL4.74(hRluc/TK) *Renilla* luciferase vector; Promega] using Lipofectoamine 2000 (Invitrogen). After 48 h of incubation, the cells were washed three times with PBS and lysed with 200 μL of lysis buffer containing 20 mM Tris, pH 7.5, 150 mM NaCl, 1 mM EDTA, 0.1% Triton X-100, and 1 mM phenylmethylsulfonyl fluoride. The lysates were centrifuged at 16 000 *g* for 5 min at 4°C and the supernatant was collected. We mixed 10 μL of the supernatant and 50 μL of firefly luciferase assay substrate buffer (50 mM Tris, pH 8.0, 5 mM $MgSO_4$, 0.5 mM CoA, 0.5 mM ATP, and 0.25 mM D-luciferin) and measured firefly luciferase activity with a luminometer (model LB9506; Berthold Technologies, Bad Wildbad, Germany). Next, *Renilla* luciferase substrate buffer (50 mM Tris, pH 8.0, 0.5 M NaCl, 10 mM EDTA, and 1 mM coelenterazine) was added to the same mixture. The assay was performed independently three times.

Immunocytochemistry

PC12 cells (8×10^5 cells) were seeded onto poly-L-lysine-coated 3.5-cm diameter dishes and co-transfected with 1.67 μg of Math2

© 2008 The Authors
Journal Compilation © 2008 International Society for Neurochemistry,

expression vector, Prg1 expression vector, or control vector and 0.33 μg of LNGFR expression vector (a transfectant marker) using Lipofectoamine2000 (Invitrogen). For the siRNA study, cells were co-transfected with 1.67 μg of Math2 expression vector, Prg1 expression vector, or control vector; 0.33 μg of LNGFR expression vector; and 25 nM Prg1 siRNA (5′-GGGCAGUAUUAGGAU AAAGTT-3′) or *Silencer* Select negative control siRNA (Applied Biosystems). Seventeen hours after transfection, cells were collected and re-seeded (3×10^5 cells) onto poly-L-lysine-coated 3.5-cm diameter dishes for real-time RT-PCR and onto poly-L-lysine-coated 2.5-cm diameter glass coverslips placed in 3.5-cm dishes for immunocytochemistry. Seven, 31, and 55 h after re-seeding, cDNA for real-time RT-PCR was prepared as described above. The other sets of cells were subjected to immunocytochemistry for morphological analyses. Cells intended for immmunohistochemistry were fixed with 4% *p*-formaldehyde (Sigma Chemical) in 0.1 M phosphate buffer for 15 min at 25°C. Cells were washed with PBS two times, permeabilized with 0.1% Triton X-100 in PBS for 5 min, and blocked with PBS containing 1% fetal calf serum for 1 h. We incubated the cells with FITC-conjugated anti-LNGFR antibody (1 : 10; Miltenyi Biotec) and rhodamine-conjugated anti-phalloidin antibody (1 : 100; Chemicon, Temecula, CA, USA) to visualize F-actin filaments in the identical field, for 15 min at 25°C. For each dish, 10–20 fluorescent images were obtained using a laser scanning confocal microscopy imaging system (Olympus, Tokyo, Japan). Fifty cells were randomly chosen from each group and analyzed. The length of individual neurites from each cell was measured using the public domain NIH program Image-J (Bethesda, MD, USA) (Rasband 1997; Abramoff *et al.* 2004; http://www.rsb.info.nih.gov/ij).

Data were presented as mean ± SEM for each group. ANOVA followed by Dunnett or Tukey–Kramer tests were used for statistical analysis of data from the Math2 and Prg1 transfection study, or the Math2 and Prg1 siRNA co-transfection study, respectively. A value of $p < 0.05$ was regarded as significant.

Results

Prg1 is induced by over-expression of Math2 in cultured cortical cells and PC12 cells

To identify the target genes of Math2, we performed gene expression analysis using DNA microarrays and cultured cortical cells transfected with either a Math2 expression vector ($n = 3$) or a control vector ($n = 3$). Transfection efficiency is extremely low in primary cell cultures. Thus, to separate the transfected cells, we co-transfected the cells with a vector expressing LNGFR, encoding the cytoplasmically truncated cell surface marker, in addition to the Math2 expression vector or control vector. The transfected cells were labeled with paramagnetic microbeads coupled to monoclonal anti-LNGFR antibody, and then separated by columns in a magnetic field. We used immunocytochemistry to confirm that transfected cortical cultures co-expressed Math2 and LNGFR (data not shown). Over 80% of the separated cultured cortical cells were found to be transfected as determined by immunocytochemistry with anti-LNGFR antibody (data not shown). Putative Math2-regulated genes were selected by using the following criteria: (i) if the gene was called 'present' in at least two of six samples; (ii) if parametric tests showed significant difference ($p < 0.05$) between two groups after the normalization method; and (iii) if the change in expression levels between two groups was greater than twofold. As a result, 46 genes – 31 up-regulated genes and 15 down-regulated genes – were identified among the 31 100 genes (see Table S1). All raw data are available at the National Center for Biotechnology Information Gene Expression Omnibus (http://www.ncbi.nlm.nih.gov/geo, accession number GSE11829).

To determine whether the 46 genes affected by Math2 over-expression correspond to specific functional classifications, we used supervised queries of the GO database. GO classified the genes into 10 main categories ($p < 0.05$; Table 1). The category showing the highest *p*-value ($p = 0.0028$) was nervous system development. The genes belonging to the nervous system development category are shown in Table 2. In this category, the gene showing the highest *p*-value was galanin; however, galanin expression levels were extremely low. Moreover, we were not able to detect any Math2-induced changes in galanin expression by real-time quantitative PCR. Thus, we focused on Prg1, the gene showing the second highest *p*-value in the nervous system development category. Prg1 up-regulation was confirmed in cultured rat cortical cells transfected with Math2. Math2 over-expression significantly increased Prg1 expression compared with the control (Fig. 1a; control: 100 ± 31.9%; Math2: 467.8 ± 122.0%). Prg1 up-regulation was also observed in Math2-transfected PC12 cells (Fig. 1b; control: 100 ± 10.3%; Math2: 152.9 ± 15.3%).

Table 1 Functional classification of genes altered by Math2 transfection[a]

Category	Number of genes	*p*-value
Nervous system development	7	0.0028
System development	7	0.0035
Protein amino acid glycosylation	3	0.0170
Biopolymer glycosylation	3	0.0174
Glycoprotein biosynthesis	3	0.0200
Cellular metabolism	18	0.0203
Negative regulation of cellular process	6	0.0256
Glycoprotein metabolism	3	0.0272
Negative regulation of biological process	6	0.0357
Metabolism	18	0.0456

[a]Gene ontology was used for functional clustering analysis. The Fisher's exact test was applied to evaluate the statistical significance of the association between the 46 genes and GO database ($p < 0.05$). GO terms are described according to the GO database (http://www.geneontology.org/). GO, gene ontology.

© 2008 The Authors
Journal Compilation © 2008 International Society for Neurochemistry,

Table 2 Genes altered by Math2 transfection in cultured rat cortical cells: nervous system development[a]

Probe ID	Fold	*p*-value	Description
1387088_at	5.07	0.027	Galanin
1379374_at	4.20	0.003	Plasticity-related gene 1
1385981_at	2.64	0.018	Plasticity-related gene 1
1397367_at	2.18	0.014	Hypothetical protein LOC689663
1372299_at	2.12	0.002	Cyclin-dependent kinase inhibitor 1C (P57)
1368003_at	0.47	0.045	Aldehyde dehydrogenase family 1, subfamily A2
1367952_at	0.44	0.023	Low-density lipoprotein receptor-related protein 2
1370551_a_at	0.43	0.009	Sema domain, transmembrane domain (TM), and cytoplasmic domain (semaphorin) 6C

[a]GO database category. GO, gene ontology.

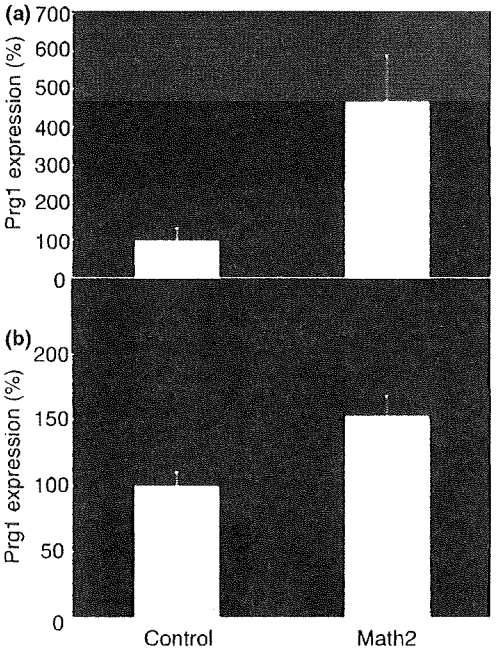

Fig. 1 Math2 transfection alters Prg1 expression. Total RNA was extracted from Math2-transfected cultured cortical cells (a) and PC12 cells (b) and was used for real-time quantitative PCR, as described in the Experimental procedures ($n = 5$). Data are given as percentage of control values (mean ± SEM). Differences were assessed using Student's t-tests; $^*p < 0.05$.

Identification of an E-box consensus sequence in the Prg1 promoter region

The bHLH transcription factors recognize and bind the consensus sequence, CANNTG, or E-box, which is located in the promoter of target genes (Massari and Murre 2000).

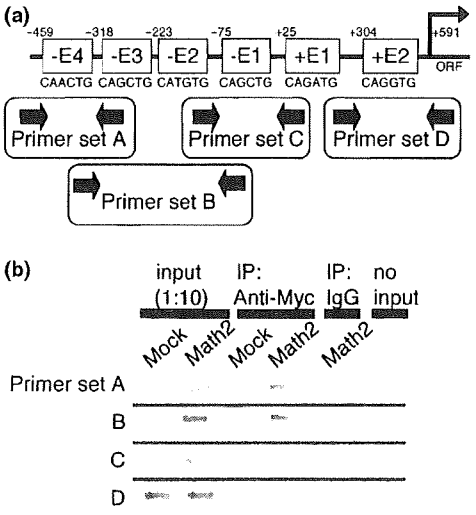

Fig. 2 Chromatin immunoprecipitation assay. (a) The location of the E-box motif and the primers used for PCR amplification after the ChIP assay. (b) DNA–protein complexes from PC12 cells transfected with control vector (Mock) or Math2 expression vector (Math2) were immunoprecipitated with anti-Myc antibody or mouse IgG antisera. The purified DNA from immunoprecipitant and non-immunoprecipitant (input, 1 : 10) was used for PCR amplification using three sets of primers for the Prg1 promoter (primer set A–C) and a set of primers for the coding region (primer set D). PCR products were electrophoresed on 2% agarose gels.

Upon analysis of the 3-kbp rat Prg1 promoter region, we found four E-boxes within 500 bp from the translation start site of Prg1. These E-boxes were designated −E1 to −E4 according to their distance from the translation start site of Prg1 (Fig. 2a). E-box consensus sequences also existed at +25 and +304 in the 5′-untranslated region; these were named +E1 and +E2, respectively (Fig. 2a).

Math2 directly binds to the Prg1 promoter region

To examine the E-boxes (−E1 to −E4) in the Prg1 promoter region that are responsible for binding to Math2, we performed ChIP assays on PC12 cells transfected with either Math2 expression vector (Math2) or control vector (Mock). Fragmented chromatin from formaldehyde cross-linked Math2 or Mock was immunoprecipitated with an antibody against the expressed tag (anti-Myc antibody). The presence of the Prg1 promoter in the immunoprecipitates was then determined by PCR and several pairs of primers (primer set A–C, Fig. 2a). As shown in Fig. 2b, the amplified Prg1 sequences obtained by using A–C primers were observed in Math2 transfectants but not in Mock cells. To test the specificity of the antibody–protein interactions, we also performed PCR on the immunoprecipitates using primers (primer set D) that recognize the Prg1 coding sequence between +265 and +492, which included +E2. No enrichment of the Prg1 coding sequence was detected in the

© 2008 The Authors

immunoprecipitates. Furthermore, non-specific IgG antibody failed to precipitate protein bound to these sequences and no bands were observed with the no-input sample (negative PCR control). A signal of the expected size can be seen in the chromatin input prior to immunoprecipitation. These results indicated that Math2 directly bound at least one of these E-boxes in the Prg1 promoter region of PC12 cells.

E1 is critical for activation by Math2

To examine which E-box was critical for the regulation of Math2-mediated Prg1 gene expression, we ligated various promoter region deletion mutants to the promoter-less luciferase reporter gene, pGL4 (luc-1445, luc-680, luc-361, luc-250, luc-176, and luc-71), as shown in Fig. 3a. Each construct, a reference vector, and Math2 expression vector or control vector were co-transfected into HEK293 cells and the luciferase activities of cell lysates were measured.

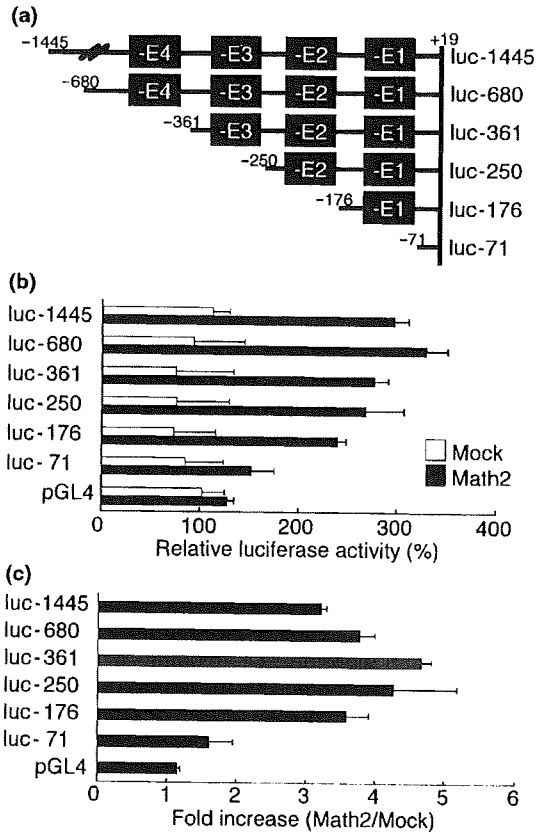

Fig. 3 The effects of Math2 on Prg1 promoter activity. (a) Different 5′-end deletion mutants of the Prg1 promoter region were ligated to a promoter-less luciferase reporter gene, pGL4 (luc-1445, luc-680, luc-361, luc-250, luc-176, and luc-71). (b) The reporter constructs, the expression vector for Math2 or control (Math2 or Mock), and reference plasmid were co-transfected into HEK293 cells. Basal-level luciferase activity of cells transfected with pGL4 and Mock was taken as 100%. Data are presented as mean ± SEM. (c) Ratio (Math2 transfection : Mock transfection) of the relative promoter activities of the upper data. Each of these experiments was repeated three times

Co-transfection with Math2 expression vector enhanced the promoter activity only when −E1 was contained within the reporter plasmid (Fig. 3b and c).

Over-expression of Math2 or Prg1 mediates neurite outgrowth in PC12 cells

The functional role of Math2 and Prg1 in PC12 cells was investigated. Twenty-four, 48, or 72 h after co-transfection with Math2 expression vector, Prg1 expression vector, or control vector and LNGFR expression vector (a transfectant marker), PC12 cells were immunofluorescently stained with anti-LNGFR antibody and anti-phalloidin antibody to visualize F-actin filaments. As shown in Fig. 4a, the neurites of Math2 transfectants and Prg1 transfectants were clearly extended 72 h after transfection compared with those of

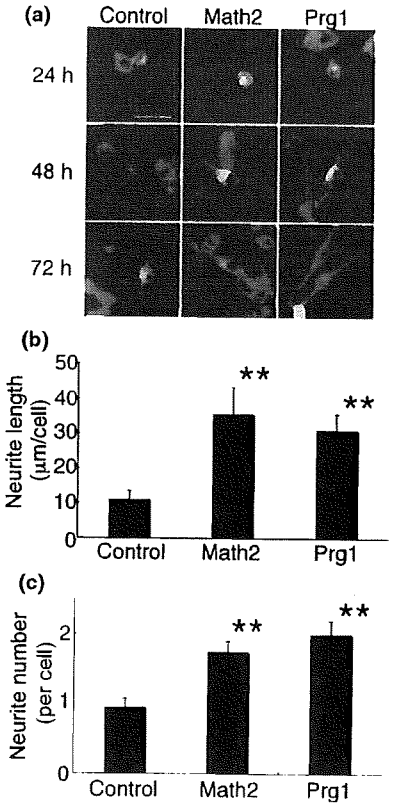

Fig. 4 The effects of Math2 or Prg1 transfection on PC12 cells. Math2, Prg1, or control and LNGFR, a transfectant marker, were co-transfected into PC12 cells. Seventeen hours after transfection, cells were collected and re-seeded. (a) Seventy-two hours after transfection, cells were double immunostained with FITC-conjugated anti-LNGFR antibody (1 : 10, green) and rhodamine-conjugated anti-phalloidin antibody (1 : 100, red) to visualize F-actin filaments. The length (b) and the number (c) of individual neurites from transfectants (double-labeled cells, yellow) were measured using Image-J. Fifty cells were randomly chosen from each group and analyzed blindly. Data are presented as mean ± SEM for each group. ANOVA followed by the Dunnett's test was used for statistical analysis; $^{**}p < 0.01$.

© 2008 The Authors
Journal Compilation © 2008 International Society for Neurochemistry,

control cells. The neurites of control cells, however, did continue to extend day by day.

Twenty-four, 48, or 72 h after transfection, we measured the length and counted the number of individual neurites from 50 randomly chosen cells using Image-J. The analysis of cells was performed blindly. The total neurite length of each cell significantly increased 72 h after transfection with Math2 or Prg1 (Fig. 4b; control: 11.1 ± 2.4 μm; Math2 transfectant: 35.6 ± 7.5 μm; Prg1 transfectant: 31.0 ± 4.6 μm; ANOVA followed by Dunnett test $p < 0.01$). The number of neurites of each cell also increased 72 h after transfection with Math2 or Prg1 (Fig. 4c; control: 0.94 ± 0.13; Math2 transfectant: 1.74 ± 0.15; Prg1 transfectant: 2.00 ± 0.19; ANOVA followed by Dunnett test $p < 0.01$). The percentage of cells that formed neurites in the control, Math2 transfectant, and Prg1 transfectant cultures were 60%, 86%, and 88%, respectively. The effect of Prg1 on neurite formation was not significantly different compared with that of Math2. On the other hand, neurite length and neurite number did not significantly change 24 or 48 h after transfection (24 h after transfection, control: 3.7 ± 0.9 μm and 0.84 ± 0.09; Math2 transfectant: 2.8 ± 0.4 μm and 0.90 ± 0.10; Prg1 transfectant: 2.9 ± 0.4 μm and 0.96 ± 0.12; 48 h after transfection, control: 11.0 ± 2.9 μm and 1.30 ± 0.17; Math2 transfectant: 14.6 ± 2.1 μm and 1.56 ± 0.18; Prg1 transfectant: 16.3 ± 2.8 μm and 1.48 ± 0.19). The soma diameter did not significantly change in any of the three groups of cells (data not shown).

Prg1 is essential for neurite outgrowth in PC12 cells induced by Math2

To examine whether the neurite outgrowth induced by Math2 occurred through Prg1, we co-transfected PC12 cells with (i) Prg1 siRNA or negative control siRNA, (ii) Math2 expression vector or control vector, and (iii) LNGFR expression vector (a transfectant marker). We selected the most effective Prg1 siRNA from three Prg1 siRNAs. The Prg1 siRNA used in this experiment inhibited 80% of endogenous Prg1 expression in PC12 cells analyzed by real-time quantitative RT-PCR (data not shown). We used immunofluorescent staining to confirm whether individual PC12 cells were successfully co-transfected with all three: siRNA, Math2 expression vector, and marker vector (data not shown). Next, we assessed Prg1 expression in the transfectants by using real-time quantitative RT-PCR. Seventy-two hours after transfection with Math2, Prg1 mRNA expression in PC12 cells was significantly increased. Co-transfection with Prg1 siRNA and Math2 significantly decreased Prg1 expression to control levels (Fig. 5a).

Changes in morphology were determined by immunofluorescent staining. As shown in Fig. 5b, the neurite of the Math2 transfectant was clearly extended 72 h after transfection compared with control cells, which is consistent with the Math2-expressing cells shown in Fig. 4a. Co-transfection with Prg1 siRNA and Math2 decreased the neurite length to control levels (Fig. 5b). Seventy-two hours after transfection, we measured the length and counted the number of individual neurites from 50 cells using Image-J. The analysis of cells was done blindly. The total neurite length of each cell significantly increased after transfection with Math2. On the other hand, co-transfection with Prg1 siRNA and Math2 significantly decreased the neurite length to control values (Fig. 5c, control vector and negative control siRNA: 12.7 ± 1.6 μm; control vector and Prg1 siRNA: 14.2 ± 2.8 μm; Math2 vector and negative control siRNA: 34.4 ± 3.8 μm; Math2 vector and Prg1 siRNA: 9.9 ± 2.1 μm; Tukey–Kramer $p < 0.05$). The number of neurites of each cell also increased 72 h after transfection with Math2. Co-transfection with Prg1 siRNA and Math2 significantly decreased the number of neurites to control values (Fig. 5d; control vector and negative control siRNA: 1.32 ± 0.16; control vector and Prg1 siRNA: 1.49 ± 0.17; Math2 vector and negative control siRNA: 1.99 ± 0.18; Math2 vector and Prg1 siRNA: 1.16 ± 0.17; Tukey–Kramer $p < 0.05$). The percentage of cells that formed neurites in cultures transfected with control vector and negative control siRNA, control vector and Prg1 siRNA, Math2 vector and negative control siRNA, and Math2 vector and Prg1 siRNA were 80%, 90%, 90%, and 62%, respectively. The soma diameter did not significantly change in any of the groups examined (data not shown).

To confirm that Prg1 siRNA specifically blocked Prg1 activity, we repeated the neurite experiment by over-expressing Prg1 and transfecting the cells with Prg1 siRNA. Seventy-two hours after transfection, the total neurite length of each cell significantly increased after transfection with Prg1. On the other hand, co-transfection with Prg1 siRNA and Prg1 significantly decreased neurite length (control vector and negative control siRNA: 8.1 ± 1.1 μm; control vector and Prg1 siRNA: 7.1 ± 1.7 μm; Prg1 vector and negative control siRNA: 19.2 ± 2.4 μm; Prg1 vector and Prg1 siRNA: 11.9 ± 1.6 μm; Tukey–Kramer $p < 0.05$). The number of neurites of each cell also significantly increased 72 h after transfection with Prg1. Co-transfection with Prg1 siRNA and Prg1 decreased the number of neurites (control vector and negative control siRNA: 1.32 ± 0.27; control vector and Prg1 siRNA: 1.11 ± 0.15; Prg1 vector and negative control siRNA: 1.79 ± 0.16; Prg1 vector and Prg1 siRNA: 1.43 ± 0.17; Tukey–Kramer $p < 0.05$). The percentage of cells that formed neurites in cultures transfected with control vector and negative control siRNA, control vector and Prg1 siRNA, Prg1 vector and negative control siRNA, and Prg1 vector and Prg1 siRNA were 66%, 70%, 68%, and 66%, respectively.

Discussion

In this study, we demonstrated that a bHLH transcription factor, Math2, regulated Prg1 expression by directly binding

© 2008 The Authors
Journal Compilation © 2008 International Society for Neurochemistry.

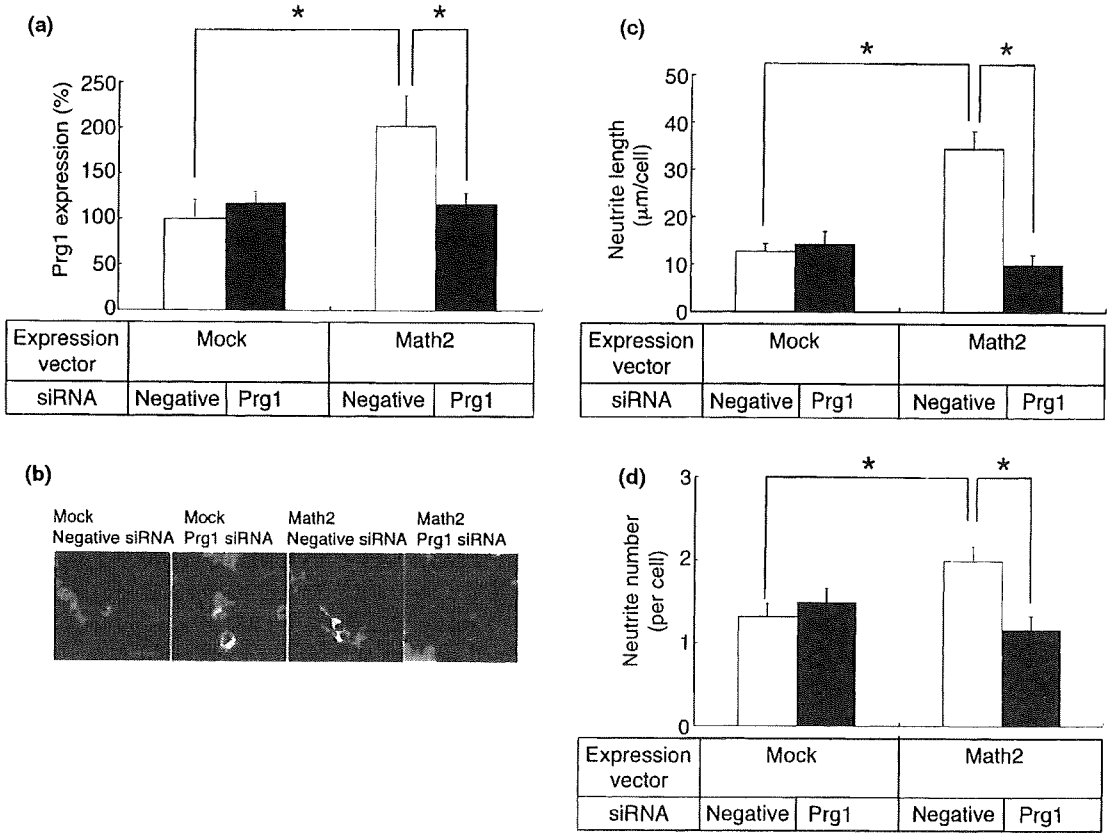

Fig. 5 The effects of Prg1 siRNA on Math2-mediated morphological changes in PC12 cells. Prg1 siRNA, Math2, and LNGFR, a transfectant marker, were co-transfected into PC12 cells. Seventeen hours after transfection, cells were collected and re-seeded. (a) Seventy-two hours after transfection, the expression of Prg1 in these cells was determined by real-time quantitative PCR. Data are presented as mean ± SEM for each group. The Tukey–Kramer method was used for statistical analysis; $^*p < 0.05$. (b) Seventy-two hours after transfection, cells were double immunostained with FITC-conjugated anti-LNGFR antibody (1 : 10, green) and rhodamine-conjugated anti-phalloidin antibody (1 : 100, red) to visualize F-actin filaments. The length (c) and the number (d) of individual neurites from the transfectants (double-labeled cells, yellow) were measured using Image-J. Fifty cells were randomly chosen from each group and analyzed blindly. Data are presented as mean ± SEM for each group. The Tukey–Kramer method was used for statistical analysis; $^*p < 0.05$.

to at least one E-box in the promoter region of Prg1. We also demonstrated that Math2 mediated neurite outgrowth through Prg1 expression.

To identify the target genes of Math2, we performed gene expression analysis using DNA microarrays and cultured cortical cells transfected with a Math2 expression vector. The 46 genes affected by Math2 over-expression were classified into 10 main GO database categories. The category showing the highest p-value ($p = 0.0028$) was nervous system development. The genes belonging to the nervous system development category were galanin, Prg1, hypothetical protein LOG689663, cyclin-dependent kinase inhibitor 1c, aldehyde dehydrogenase family, low-density lipoprotein receptor-related protein 2, and semaphorin 6c (Table 2; Prg1 is listed twice, each with different probe IDs. Both IDs refer to Prg1). PC12 cells that constitutively express Nex1 (Math2) have undergone gene expression profiling (Uittenbogaard and Chiaramello 2004). The genes affected by constitutive over-expression of Nex1 (Math2) were categorized as cytoskeletal genes, cell adhesion encoding genes, vesicular trafficking/synapse-related genes, metabolic-related genes, stress response-related genes, mitochondrial genes, and transcription factor and chromatin-related genes. Although the cells, microarrays, and categorization methods used by Uittenbogaard and Chiaramello were different from ours, several categories and genes were identical. For example, both our group and Uittenbogaard and Chiaramello observed that Math2 expression affected the expression of the gene for the inhibitor of the cyclin-dependent kinase 4 (INK4) family, which plays a role in promoting cell-cycle arrest.

In this study, we focused on Prg1, which belongs to the nervous system development category. Prg1 was initially identified as a lipid phospholipid phosphatase (LPP) that is specifically expressed in neurons (Brauer *et al.* 2003). *In situ* hybridization analysis showed that Prg1 mRNA appears in the hippocampus starting on E19 and remains present in the

© 2008 The Authors
Journal Compilation © 2008 International Society for Neurochemistry,

hippocampus and also in the entorhinal cortex from the day of birth to adulthood. Induction of Prg1 was observed after lesioning the entorhinal cortex, which leads to a layer-specific denervation of the hippocampus followed by regenerative ingrowth of sprouting axons (Deller *et al.* 1995; Savaskan and Nitsch 2001). On the other hand, Math2 mRNA is not detectable on E12 but becomes abundant on E16, a developmental stage in rodents when large numbers of post-mitotic neurons are generated (Angevine and Sidman 1961). The highest steady state level of Math2 mRNA occurs during the first postnatal week, after which transcripts decrease but remain at stable levels into adulthood (Bartholoma and Nave 1994). The similarity between Math2 and Prg1 expression profiles raised the possibility that Math2 controls Prg1, the latter of which is not only involved in neuronal outgrowth and sprouting (synaptogenesis) during late developmental stages but also in synaptic plasticity and maintenance of the differentiated state throughout adulthood.

We examined the promoter region of Prg1 and found four E-boxes within 500 bp from the translation start site of Prg1. Using ChIP assays, we found that Math2 directly bound to at least one of these E-boxes. We then examined which E-box was critical for the regulation of Prg1 gene expression by Math2. In this experiment, we used HEK293 cells, because they express very little, if any, endogenous Math2; thus, the effect of Math2 could be easily detected.

Next, we investigated the functional role of Math2 and Prg1 in PC12 cells. Seventy-two hours after transfection with Math2 or Prg1, the total length and the number of neurites of each cell significantly increased. To examine whether the neurite outgrowth induced by Math2 occurred through Prg1, we co-transfected PC12 cells with (i) Prg1 siRNA or negative control siRNA, (ii) Math2 expression vector or control vector, and (iii) LNGFR expression vector (a transfectant marker). Seventy-two hours after transfection with Math2, Prg1 mRNA expression in PC12 cells was significantly increased. Co-transfection with Prg1 siRNA and Math2 significantly decreased Prg1 expression to control levels (Fig. 5a). However, Prg1 siRNA did not decrease endogenous levels of Prg1 in Mock-transfected cells.

We screened the inhibitory effects of three Prg1 siRNAs on endogenous Prg1 expression in PC12 cells using real-time RT-PCR. One siRNA that we used in this study inhibited 80% of endogenous Prg1 expression compared with negative siRNA transfectants. The condition of cells (e.g. cell density, passage of culture, or the state of differentiation) is known to induce changes in the expression levels of various genes. Thus, we suspect that the different inhibitory effects we observed between the siRNAs during the screening and during the experiments may be due to varying endogenous Prg1 expression levels caused by the condition of the PC12 cells. In fact, Prg1-to-β-actin ratios in the siRNA experiments were lower than those in the screening experiment. Thus, we concluded that we could not detect the inhibitory effect due to the low level of endogenous Prg1 expression.

Prg1 has been reported to dephosphorylate extracellular phospholipid lysophosphatidic acid (LPA) (Brauer *et al.* 2003). LPA causes rapid neurite retraction and subsequent cell rounding through its specific receptor (Jalink *et al.* 1994). However, Prg1 over-expression inhibits the LPA-mediated neurite retraction in N1E115 cells (Brauer *et al.* 2003). Taken together, these observations suggest that the mechanisms underlying Math2–Prg1-mediated neurite outgrowth may involve the LPA signal transduction system.

In summary, we demonstrated that a bHLH transcription factor, Math2, regulates Prg1 expression by directly binding to at least one of four E-boxes in the promoter region of Prg1. We also showed that Math2 mediates neurite outgrowth through Prg1 expression. Our results suggest that the Math2–Prg1 cascade mediates neuronal maturation, reorganization, and plastic changes in the nervous system.

Acknowledgements

This work was in part supported by Research Grants from the Ministry of Health, Labour and Welfare of Japan; the Ministry of Education, Culture, Sport, Science and Technology of Japan; and the Japan Society for the Promotion of Science.

Supporting information

Additional supporting information may be found in the online version of this article.

Table S1 Genes altered by transfecting Math2 into rat cultured cortical cells.

Please note: Blackwell Publishing are not responsible for the content or functionality of any supporting information supplied by the authors. Any queries (other than missing material) should be directed to the corresponding author for the article.

References

Abramoff M. D., Magelhaes P. J. and Ram S. J. (2004) Image processing with ImageJ. *Biophotonics Int.* **11**, 36–42.

Akazawa C., Sasai Y., Nakanishi S. and Kageyama R. (1992) Molecular characterization of a rat negative regulator with a basic helix-loop-helix structure predominantly expressed in the developing nervous system. *J. Biol. Chem.* **267**, 21879–21885.

Angevine J. B. Jr and Sidman R. L. (1961) Autoradiographic study of cell migration during histogenesis of cerebral cortex in the mouse. *Nature* **192**, 766–768.

Bartholoma A. and Nave K. A. (1994) NEX-1: a novel brain-specific helix-loop-helix protein with autoregulation and sustained expression in mature cortical neurons. *Mech. Dev.* **48**, 217–228.

Brauer A. U., Savaskan N. E., Kuhn H., Prehn S., Ninnemann O. and Nitsch R. (2003) A new phospholipid phosphatase, PRG-1, is involved in axon growth and regenerative sprouting. *Nat. Neurosci.* **6**, 572–578.

Deller T., Frotscher M. and Nitsch R. (1995) Morphological evidence for the sprouting of inhibitory commissural fibers in response to the

© 2008 The Authors
Journal Compilation © 2008 International Society for Neurochemistry,

lesion of the excitatory entorhinal input to the rat dentate gyrus. *J. Neurosci.* **15**, 6868–6878.

Dennis G. Jr, Sherman B. T., Hosack D. A., Yang J., Gao W., Lane H. C. and Lempicki R. A. (2003) DAVID: database for annotation, visualization, and integrated discovery. *Genome Biol.* **4**, P3.

Duncan M., DiCicco-Bloom E. M., Xiang X., Benezra R. and Chada K. (1992) The gene for the helix-loop-helix protein, Id, is specifically expressed in neural precursors. *Dev. Biol.* **154**, 1–10.

Farah M. H., Olson J. M., Sucic H. B., Hume R. I., Tapscott S. J. and Turner D. L. (2000) Generation of neurons by transient expression of neural bHLH proteins in mammalian cells. *Development* **127**, 693–702.

Feder J. N., Jan L. Y. and Jan Y. N. (1993) A rat gene with sequence homology to the *Drosophila* gene hairy is rapidly induced by growth factors known to influence neuronal differentiation. *Mol. Cell. Biol.* **13**, 105–113.

Hubbell E., Liu W. M. and Mei R. (2002) Robust estimators for expression analysis. *Bioinformatics* **18**, 1585–1592.

Ishibashi M., Sasai Y., Nakanishi S. and Kageyama R. (1993) Molecular characterization of HES-2, a mammalian helix-loop-helix factor structurally related to *Drosophila* hairy and Enhancer of split. *Eur. J. Biochem.* **215**, 645–652.

Jalink K., van Corven E. J., Hengeveld T., Morii N., Narumiya S. and Moolenaar W. H. (1994) Inhibition of lysophosphatidate- and thrombin-induced neurite retraction and neuronal cell rounding by ADP ribosylation of the small GTP-binding protein Rho. *J. Cell Biol.* **126**, 801–810.

Johnson J. E., Birren S. J. and Anderson D. J. (1990) Two rat homologues of *Drosophila* achaete-scute specifically expressed in neuronal precursors. *Nature* **346**, 858–861.

Kageyama R., Ishibashi M., Takebayashi K. and Tomita K. (1997) bHLH transcription factors and mammalian neuronal differentiation. *Int. J. Biochem. Cell Biol.* **29**, 1389–1399.

Lee J. E. (1997) Basic helix-loop-helix genes in neural development. *Curr. Opin. Neurobiol.* **7**, 13–20.

Massari M. E. and Murre C. (2000) Helix-loop-helix proteins: regulators of transcription in eucaryotic organisms. *Mol. Cell. Biol.* **20**, 429–440.

Neuman T., Keen A., Zuber M. X., Kristjansson G. I., Gruss P. and Nornes H. O. (1993) Neuronal expression of regulatory helix-loop-helix factor Id2 gene in mouse. *Dev. Biol.* **160**, 186–195.

Nieto M., Schuurmans C., Britz O. and Guillemot F. (2001) Neural bHLH genes control the neuronal versus glial fate decision in cortical progenitors. *Neuron* **29**, 401–413.

Rasband W. S. (1997-2007) *ImageJ*. U. S. National Institutes of Health, Bethesda, MD

Sakagami T., Sakurada K., Sakai Y., Watanabe T., Nakanishi S. and Kageyama R. (1994) Structure and chromosomal locus of the mouse gene encoding a cerebellar Purkinje cell-specific helix-loop-helix factor Hes-3. *Biochem. Biophys. Res. Commun.* **203**, 594–601.

Sasai Y., Kageyama R., Tagawa Y., Shigemoto R. and Nakanishi S. (1992) Two mammalian helix-loop-helix factors structurally related to *Drosophila* hairy and Enhancer of split. *Genes Dev.* **6**, 2620–2634.

Savaskan N. E. and Nitsch R. (2001) Molecules involved in reactive sprouting in the hippocampus. *Rev. Neurosci.* **12**, 195–215.

Schwab M. H., Bartholomae A., Heimrich B. *et al.* (2000) Neuronal basic helix-loop-helix proteins (NEX and BETA2/Neuro D) regulate terminal granule cell differentiation in the hippocampus. *J. Neurosci.* **20**, 3714–3724.

Shimizu C., Akazawa C., Nakanishi S. and Kageyama R. (1995) MATH-2, a mammalian helix-loop-helix factor structurally related to the product of *Drosophila* proneural gene atonal, is specifically expressed in the nervous system. *Eur. J. Biochem.* **229**, 239–248.

Sun Y., Nadal-Vicens M., Misono S., Lin M. Z., Zubiaga A., Hua X., Fan G. and Greenberg M. E. (2001) Neurogenin promotes neurogenesis and inhibits glial differentiation by independent mechanisms. *Cell* **104**, 365–376.

Takebayashi K., Akazawa C., Nakanishi S. and Kageyama R. (1995) Structure and promoter analysis of the gene encoding the mouse helix-loop-helix factor HES-5. Identification of the neural precursor cell-specific promoter element. *J. Biol. Chem.* **270**, 1342–1349.

Tomita K., Moriyoshi K., Nakanishi S., Guillemot F. and Kageyama R. (2000) Mammalian achaete-scute and atonal homologs regulate neuronal versus glial fate determination in the central nervous system. *EMBO J.* **19**, 5460–5472.

Uittenbogaard M. and Chiaramello A. (2002) Constitutive overexpression of the basic helix-loop-helix Nex1/MATH-2 transcription factor promotes neuronal differentiation of PC12 cells and neurite regeneration. *J. Neurosci. Res.* **67**, 235–245.

Uittenbogaard M. and Chiaramello A. (2004) Expression profiling upon Nex1/MATH-2-mediated neuritogenesis in PC12 cells and its implication in regeneration. *J. Neurochem.* **91**, 1332–1343.

Uittenbogaard M. and Chiaramello A. (2005) The basic helix-loop-helix transcription factor Nex-1/Math-2 promotes neuronal survival of PC12 cells by modulating the dynamic expression of anti-apoptotic and cell cycle regulators. *J. Neurochem.* **92**, 585–596.

Wu S. X., Goebbels S., Nakamura K., Nakamura K., Kometani K., Minato N., Kaneko T., Nave K. A. and Tamamaki N. (2005) Pyramidal neurons of upper cortical layers generated by NEX-positive progenitor cells in the subventricular zone. *Proc. Natl Acad. Sci. USA* **102**, 17172–17177.

Yamada M., Kiuchi Y., Nara K., Kanda Y., Morinobu S., Momose K., Oguchi K., Kamijima K. and Higuchi T. (1999) Identification of a novel splice variant of heat shock cognate protein 70 after chronic antidepressant treatment in rat frontal cortex. *Biochem. Biophys. Res. Commun.* **261**, 541–545.

Yamada M., Yamada M., Yamazaki S. *et al.* (2000) Identification of a novel gene with RING-H2 finger motif induced after chronic antidepressant treatment in rat brain. *Biochem. Biophys. Res. Commun.* **278**, 150–157.

© 2008 The Authors
Journal Compilation © 2008 International Society for Neurochemistry,

BRAIN RESEARCH 1208 (2008) 160–169

available at www.sciencedirect.com

ScienceDirect

www.elsevier.com/locate/brainres

BRAIN RESEARCH

Research Report

Antidepressant-like effects of the delta-opioid receptor agonist SNC80 ([(+)-4-[(alphaR)-alpha-[(2S,5R)-2, 5-dimethyl-4-(2-propenyl)-1-piperazinyl]-(3-methoxyphenyl) methyl]-N,N-diethylbenzamide) in an olfactory bulbectomized rat model

Akiyoshi Saitoh[a,*], *Mitsuhiko Yamada*[b], *Misa Yamada*[b], *Kou Takahashi*[b], *Kazumasa Yamaguchi*[c], *Hiroyasu Murasawa*[c], *Akiko Nakatani*[c], *Yoshimi Tatsumi*[d], *Noritaka Hirose*[a], *Junzo Kamei*[a]

[a]*Department of Pathophysiology & Therapeutics, School of Pharmacy and Pharmaceutical Sciences, Hoshi University, 4-41 Ebara 2-chome, Shinagawa-ku, Tokyo 142-8501, Japan*
[b]*Department of Psychogeriatrics, National Institute of Mental Health, National Center of Neurology and Psychiatry, Tokyo 187-8502, Japan*
[c]*Department of Pharmacology, Nihon Bioresearch Inc., 6-104 Majima, Fukuju-cho, Hashima, Gifu 501-6251, Japan*
[d]*Narabyouri Research Co., Ltd. 2631-82, Tsuge Hayama-cho, Nara, 632-0231, Japan*

ARTICLE INFO

Article history:
Accepted 5 July 2007
Available online 4 September 2007

Keywords:
Olfactory bulbectomy
Delta opioid receptor
Antidepressant
Anxiety
Depression
SNC80

ABSTRACT

The responses of olfactory bulbectomized (OBX) rats to antidepressant treatment are similar to those of depressed patients since chronic administration of an antidepressant reverses OBX-induced behavioral and physiological changes. Previously, using several animal models, it was demonstrated that single treatment with delta-opioid receptor agonists produced an antidepressant-like effect. This study examined the antidepressant effects resulting from subchronic exposure for 8 days to the delta-opioid receptor agonist SNC80 in an OBX rat model of depression. The olfactory bulbs were removed by suction. The emotionality of rats was measured by scoring their responses to given stimuli, i.e., attack, startle, struggle, and fight responses. The OBX rats chronically treated with vehicle for 7 days at 14 days following surgery showed a significant increase in emotionality score and a decrease in the time spent and entries in the open arm of a plus-maze. In the case of OBX rats, these changes were dose- and time-dependently reversed by chronic SNC80 treatment (1–10 mg/kg, s.c.) for 7 days, as same as desipramine (10 mg/kg, i.p.). Moreover, the concentration of 5-HT and its metabolite 5-HIAA in the frontal cortex, hippocampus, and amygdala were decreased in OBX rats, and these changes were also normalized by SNC80 treatment, rather than desipramine treatment. In addition, SNC80 also significantly reversed the loss of TH-positive cells produced by OBX in the dorsal raphe. In conclusion, we demonstrated that subchronic SNC80 treatment could completely reverse OBX-induced behavioral abnormalities and defects in serotonergic function.

© 2007 Published by Elsevier B.V.

* *Corresponding author.* Fax: +81 3 5498 5745.
E-mail address: a-saitoh@hoshi.ac.jp (A. Saitoh).

0006-8993/$ – see front matter © 2007 Published by Elsevier B.V.
doi:10.1016/j.brainres.2007.07.095

1. Introduction

Several lines of evidence have suggested the involvement of the opioid system in the mechanisms underlying the physiopathology of depression and the action of antidepressants. Recent studies with knockout mice that lack delta-opioid receptors (Filliol et al., 2000) or preproenkephalin-derived peptides (Konig et al., 1996; Ragnauth et al., 2001) revealed that both types of knockout mice showed high anxiety levels. In addition, compounds that the delta-opioid receptor agonists have been shown to have antidepressant-like properties in several animal models. The selective delta-opioid agonist Tyr-$_D$-Ser-(O-C(CH_3)$_3$)-Gly-Phe-Leu-Thr-(O-C(CH_3)$_3$ produced antidepressant-like effects in the learned helplessness model of depression (Tejedor-Real et al., 1998). Similarly, the treatment with enkephalinase inhibitors such as RB101 was associated with antidepressant-like effects in mice and rat models of depression (Baamonde et al., 1992; Tejedor-Real et al., 1998). More recently, the nonpeptidic delta-opioid agonists (+)-4-[α(*R*)-α-[(2*S*,5*R*)-2,5-dimethyl-4-(2-propenyl)-1-piperazinyl]-(3-hydroxyphenyl)methyl]-*N*,*N*-diethylbenzamide [(+)BW373U86] and (+)-4-[(aR)-a-((2*S*,5*R*)-4-allyl-2,5-dimethyl-1piperazinyl)-3-methoxybenzyl]-*N*,*N*-diethylbenzamide (SNC80) have been shown to produce antidepressant- and anxiety-like effects in several rodent models (Broom et al., 2002; Jutkiewicz et al., 2004, 2005a,b; Saitoh et al., 2004, 2006; Torregrossa et al., 2005, 2006; Perrine et al., 2006). We also demonstrated that single treatment with delta-opioid receptor agonists inhibited the depressant- and anxiety-like behavior in mice and rats using forced-swim test, conditioned-fear stress test, and elevated plus-maze test, on the contrary delta-opioid receptor antagonists produce anxiety-like behavior in rats in the elevated plus-maze test (Saitoh et al., 2004, 2005). Overall, these findings suggest that the delta-opioid receptor system may be related to depression or anxiety.

The following behavioral abnormalities have been observed following bilateral olfactory bulbectomy: stress-induced increase in locomotor activity and increases in various measures of irritability or hyperemotionality to given stimuli (Thorne and Rowles, 1988; Redmond et al., 1997; Okuyama et al., 1999; Ho et al., 2001, 2004; Saitoh et al., 2003, 2006, 2007 Chaki et al., 2004). It has been reported that OBX-induced behavioral abnormalities are reversed by chronic administration of a wide range of clinically effective antidepressant drugs, including selective serotonin reuptake inhibitors (SSRIs) and serotonin and noradrenaline reuptake inhibitors (SNRIs) (for a review, see Kelly et al., 1997; Song and Leonard, 2005). These reports suggest that impairment of the central serotonergic system may play an important role in mediating the behavioral changes observed following OBX. In addition, using autoradiographic method, it was reported that the decrease in 5-HT synthesis enzyme in dorsal raphe observed in the OBX rats and lower 5-HT synthesis rates in OBX rats was reversed by the chronic treatment with SSRI citalopram (Watanabe et al., 2003; Hasegawa et al., 2005). Previously, it was reported that many types of neurotransmitter contents were decreased in OBX animals. Specifically, it was demonstrated that an imbalance in the serotonergic system is observed in the OBX syndrome since there have been consistent observations of abnormal 5-HT concentration/synthesis and receptor expression throughout the limbic system (Lumia et al., 1992; Zhou et al., 1998; Watanabe et al., 2003). Indeed, many investigators demonstrated that behavioral and neurochemical changes induced by OBX were attenuated by chronic (but not acute) antidepressant treatment (see review Song and Leonard, 2005). Thus, it has been suggested that the OBX syndrome is a useful model for detecting antidepressant activity since many of the behavioral and neurotransmitter changes observed in OBX are qualitatively similar to those observed in depressed patients.

Previously, it was reported that the OBX procedure decreased the time spent in the open arm of a plus-maze, and this behavioral changes were significantly reversed by treatment with antidepressants and anxiolytic agents for 7 days (Yamaguchi et al., 2002). Similarly, we also reported that in comparison with sham-operated rats, OBX rats exhibited hyperemotionality score and a decrease in the time spent in the open arm of a plus-maze; these behavioral changes were attenuated by subchronic 7 day treatment with the antidepressant desipramine (Saitoh et al., 2003, 2007). Thus, the evaluation of hyperemotionality and the time spent in the open arms of a plus-maze in OBX rats may provide a suitable model for evaluating antidepressants.

No previous study has tried to demonstrate the antidepressant activity by subchronic administration of delta-opioid receptor agonists using an animal model of depression. Thus, we investigated the effects of subchronic administration of SNC80 on the hyperemotionality and the time spent in the open arms of a plus-maze in OBX rats. Furthermore, to clarify the mechanism of action of SNC80, we examined the changes in the amounts of 5-HT and its metabolite 5-HIAA in OBX rat brains after subchronic SNC80 treatment and the effects of chronic SNC80

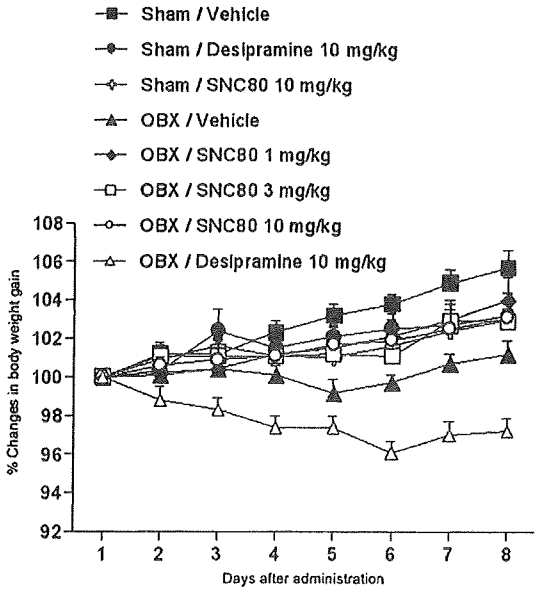

Fig. 1 – Changes in the body-weight gain of OBX and sham-operated rats that were chronically (i.p.) treated with SNC80 or desipramine. The weight of each rat was recorded daily prior to injection of the test compound. The percent changes in body-weight gain are expressed as the mean ± S.E.M. on each day. The percent changes in the body-weight gain of SNC80-treated rats did not differ significantly from those of vehicle-treated rats. The percent changes in the body-weight gain of vehicle-treated rats differed significantly from those of vehicle-treated rats on days 4 to 8.

treatments on 5-HT synthesis in OBX rats, using antibodies against tryptophan hydroxylase (TH), rate-limiting enzyme of 5-HT synthesis.

2. Results

2.1. *Changes in the body-weight gain of OBX and sham rats that were chronically treated with SNC80 or desipramine*

The average weight of each group of animals on day 1 was as follows: sham/vehicle, 330±10.9 g; sham/desipramine, 320±4.5 g; sham/SNC80 (10 mg/kg), 339.2±10.8 g; OBX/vehicle, 324±6.3 g; OBX/SNC80 (1 mg/kg), 312±7.2 g; OBX/SNC80 (3 mg/kg), 312±8.8 g; OBX/SNC80 (10 mg/kg), 323±6.4 g; and OBX/desipramine, 312±7.9 g.

Rats received injections of 1–10 mg/kg SNC80 and 10 mg/kg desipramine daily for 8 days and were weighed every day. Fig. 1 shows the average percent changes in body-weight gain for each group of animals over the course of 8 days of treatment. There were no differences between the sham and SNC80 (1 and 10 mg/kg)-treated OBX groups in terms of the percent changes in body weight on any treatment day. Rats that received SNC80 (3 mg/kg) showed changes that were similar to those in SNC80 (1 and 10 mg/kg)-treated OBX rats but were significantly different from those in sham rats on days 6 and 8. In contrast, OBX rats that received desipramine for 8 days lost weight, and the average percent changes in body-weight gain were significantly different from those in sham rats from days 2 to 8.

2.2. *Changes in olfactory bulbectomy-induced hyperemotionality in rats after subchronic SNC80 treatment*

The changes in the total responses of OBX rats are shown in Fig. 2. Fig. 2 shows that the total emotional responses of OBX rats prior to treatment were significantly higher than those of sham-operated rats at 14 days postsurgery. In addition, these emotional responses of OBX rats were not significantly affected by the vehicle after subchronic administration for 7 days. Two-way (drugs and days) factorial ANOVA revealed a significant main effect for the drugs×days interaction [drugs×days interaction: $F(8,90)=4.521$, $P<0.01$]. A post hoc test analysis showed that desipramine and higher doses of SNC80 (3 and 10 mg/kg) produced a significant decrease in the struggle response of OBX rats on day 3. A lower dose of SNC80 (1 mg/kg) also significantly decreased the total emotional response score of OBX rats on days 5 and 7. Furthermore, the inhibitory effects of SNC80 (10 mg/kg) on OBX-induced hyperemotional responses on day 7 were significantly greater than those induced by desipramine. There were no significant effects in the total emotional responses between vehicle-desipramine- and SNC80-treated sham rats (Fig. 2).

Table 1 – Effects of SNC80 and desipramine on the entries into the open/closed arm (total arm entry), closed arm or open arm in OBX rats placed for 5 min in the elevated plus-maze

Group	Dose (mg/kg, i.p.)	Closed arm entry counts	Open arm entry counts	Total arm entry counts
Sham/vehicle	–	11.1±1.4	10.4±1.4	21.6±2.7
Sham/ desipramine	10	8.8±1.5	8.0±1.8	16.8±3.3
Sham/SNC80	10	8.3±1.4	6.7±1.5	15.0±2.8
OBX/vehicle	–	1.3±0.2#	0.3±0.2#	1.6±0.4#
	1	4.7±1.6	3.7±1.6	8.4±3.1
OBX/SNC80	3	7.7±0.8*	6.9±0.7*	14.6±1.6*
	10	5.9±1.1*	5.0±1*	10.9±2.1*
OBX/ desipramine	10	3.4±0.6	2.4±0.6	5.9±1.3

Data are expressed as means±SEM ($n=7$).
#$P<0.05$ vs. sham-operated rats. *$P<0.05$ vs. vehicle-treated OB rats.

2.3. *Effects of subchronic SNC80 treatment on the elevated plus-maze test in OBX rats*

In comparison with sham-operated vehicle rats, OBX rats that had been subchronically treated with the vehicle showed a significant decrease in the number of entries into the open and closed areas (Table 1). Furthermore, they showed a decrease in the percentage of time spent in the open arms and the number of

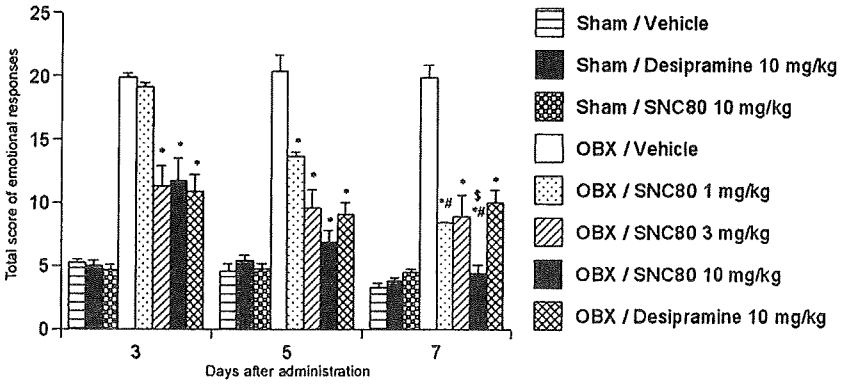

Fig. 2 – Effects of chronic antidepressant treatment on the hyperemotionality of OBX rats. Drugs (10 mg/kg i.p.) were administered chronically once daily for 7 days. Each emotional response (attack, startle, struggle, and fight) was measured 2 h after the administration of the drug on day 7. The total emotional response score is the sum of each score. Data represent mean±S.E.M. of 8 rats. *$P<0.01$ vs. vehicle-treated OBX rats. #$P<0.01$ vs. respective drug-treated OBX rats on day 1. $$P<0.05$ vs. desipramine-treated OBX rats.

entries into the open arms (Fig. 3). In comparison with vehicle-treated OBX rats, those treated with SNC80 produced significant increases in the number of entries into the closed and open areas and the total number of arm entries [total arm entries: $F(4,30)=6.614$, $P<0.01$; closed arm: $F(4,30)=6.181$, $P<0.01$; and open arm: $F(4,30)=7.056$, $P<0.01$] (Table 1). Post hoc analysis showed that the percentage of time spent in the open arms and the number of entries into the open arms by OBX rats were significantly increased by subchronic SNC80 treatment at doses of 3 and 10 mg/kg. Similar results regarding the percentage of time spent in the open arms and the number of entries into the open arms were obtained for desipramine (10 mg/kg)-treated OBX rats [% time spent in the open arms: $F(4,30)=4.229$, $P<0.01$ and % open arm entries: $F(4,30)=14.556$, $P<0.01$] (Fig. 3). However, desipramine did not significantly affect the number of entries into the total, open, or closed arms. There were no significant effects in the percentage of time spent in the open arms and the number of entries into the open arms between vehicle-, desipramine-, and SNC80-treated sham rats (Fig. 3).

2.4. *Effects of subchronic treatment of OBX rats with SNC80 on the concentrations of 5-HT and its metabolite in various brain regions*

The effects of treatment of OBX rats with SNC80 on the regional concentrations of 5-HT and its metabolite are shown in Table 2. The OBX procedure significantly decreased the 5-HT content in the frontal cortex (−12.1%), hippocampus (−55.2%), and amygdala (−49.0%) and increased the 5-HT content in the hypothalamus (+290%) of vehicle-treated OBX rats relative to sham-operated rats. On the other hand, this procedure significantly decreased the amount of 5-HIAA, the major metabolite of 5-HT, in the hippocampus (−35.4%) and amygdala (−30.9%).

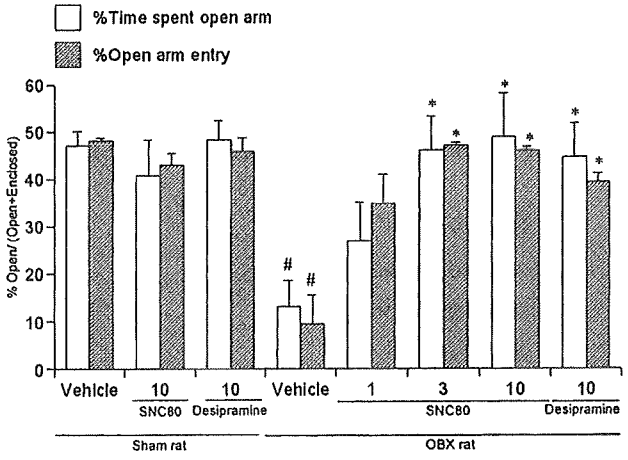

Fig. 3 – Effects of chronic SNC80 treatment on the percentage of time spent (open column) in and the number of entries (shaded column) into the open arms of an elevated plus-maze in which rats were placed for 5 min. SNC80 and desipramine were administered chronically once daily for 8 days. The elevated plus-maze test was performed 2 h after the final administration (day 8). Data represent mean ± S.E.M. of 8 rats. #P<0.01 vs. sham-operated rats. *P<0.01 vs. vehicle-treated OBX rats.

Treatment of OBX rats with SNC80 significantly reversed the decrease in the amount of 5-HT in the frontal cortex, hippocampus, and amygdala and he increase in the amount of 5-HT in the hypothalamus [frontal cortex: $F(4,29)=3.650$, $P<0.01$; hippocampus: $F(4,29)=18.538$, $P<0.01$; hypothalamus: $F(4,29)=20.068$, $P<0.01$; and amygdala: $F(4,29)=25.284$, $P<0.05$]. Similarly, the decrease in the amounts of 5-HIAA in the hippocampus, hypothalamus, and amygdala was significantly reversed by treatment with SNC80 [hippocampus: $F(4,29)=7.208$, $P<0.01$; hypothalamus: $F(4,29)=6.122$, $P<0.01$; and amygdala: $F(4,29)=13.941$, $P<0.05$].

The treatment of OBX rats with desipramine significantly reversed the decrease in the amount of 5-HT in the amygdala and the increase in the amount of 5-HT in the hypothalamus and significantly reversed the decrease in the amount of 5-HIAA in the amygdala.

2.5. *Effects of subchronic treatment of OBX rats with SNC80 on the number of tryptophane hydroxylase-positive cells in dorsal or median raphe*

Most of the tryptophane hydroxylase (TH)-positive cells are located in the dorsal raphe rather than the median raphe of the midbrain (Figs. 4A, B). The OBX procedure significantly decreased TH-positive cells in the dorsal raphe of vehicle-treated OBX rats relative to sham-operated rats [$F(3,36)=46.432$, $P<0.001$] (Fig. 4B). Subchronic treatment with SNC80 and desipramine significantly reversed the decrease in TH-positive cells produced by OBX in the dorsal raphe (Fig. 4B). There was no significant difference in the effects on TH immunoreactivity in the median raphe of OBX rats between respective treatment groups (Figs. 4A, B).

3. Discussion

In the present study, we observed the characteristics of hyperemotionality in rats 2 weeks after OBX, being associated with a significant decrease in the number of entries and time spent on the platform or in the open arm of a plus-maze. On the contrary, the time spent in the closed arm was higher in OBX rats than in sham rats. In addition, it was shown that the behavioral changes observed in OBX rats were completely reversed by subchronic desipramine treatment (10 mg/kg). These results are consistent with those reported previously (Shibata et al., 1984; Yamaguchi et al., 2002; Saitoh et al., 2003, 2007).

We also found that a higher dose of SNC80 showed a similar significant decrease in each hyperemotional response (struggle, fight, attack, and startle) of OBX rats on day 7. Furthermore, as reflected by the total score of hyperemotional responses on day 7, we demonstrated that the inhibitory effects of SNC80 (10 mg/kg) were significantly greater than those of desipramine and that treatment with SNC80 completely reversed this trend to the same level in both OBX and sham rats. Furthermore, it was shown that subchronic treatment of OBX rats with SNC80 completely reversed the decrease in the percentage of time spent in the open arm of a plus-maze. On the other hand, we demonstrated that SNC80 showed the greater inhibition of hyperemotionality scores of OBX rats on

Table 2 – Effects of subchronic treatment with SNC80 on 5-HT and its metabolite 5-HIAA in the OBX rat frontal cortex, hippocampus, hypothalamus and amygdala

Brain region	Group	Dose	(ng/g wet tissue)		5-HT ratio
			5-HT	5-HIAA	(5-HIAA/5-HT)
Frontal cortex	Sham/vehicle	–	672.23±15.33	174.81±7.290	0.261±0.013
	Sham/desipramine	10	654.16±31.32	171.86±3.69	0.270±0.02
	Sham/SNC80	10	674.93±30.77	179.62±9.16	0.268±0.015
	OBX/vehicle	–	590.54±19.68#	218.25±21.25	0.367±0.032#
		1	731.13±19.07*	213.96±16.86	0.292±0.018
	OBX/SNC80	3	669.71±35.13	158.37±14.29	0.236±0.015*
		10	711.53±38.45*	202.29±15.67	0.282±0.010
	OBX/desipramine	10	644.51±29.43	207.94±18.20	0.322±0.021
Hippocampus	Sham/vehicle	–	521.10±34.79	237.79±15.28	0.460±0.023
	Sham/desipramine	10	546.62±30.36	259.7±17.05	0.475±0.017
	Sham/SNC80	10	514.49±32.97	243.76±17.45	0.479±0.036
	OBX/vehicle	–	233.40±16.40#	153.63±13.31#	0.669±0.056
		1	556.22±21.78*	273.91±15.26*	0.487±0.021
	OBX/SNC80	3	409.63±34.76*	194.56±24.32	0.491±0.046
		10	451.27±54.30*	260.62±31.33*	0.604±0.031
	OBX/desipramine	10	252.90±14.45	159.42±14.26	0.639±0.060
Hypothalamus	Sham/vehicle	–	474.60±43.54	219.07±31.47	0.449±0.030
	Sham/desipramine	10	469.92±37.05	200.34±10.29	0.434±0.032
	Sham/SNC80	10	467.50±34.41	225.77±24.13	0.479±0.024
	OBX/vehicle	–	1376.42±169.14#	194.3±23.63	0.142±0.010#
		1	576.67±23.96*	294.59±29.93*	0.507±0.035*
	OBX/SNC80	3	749.32±44.22*	248.72±19.82	0.330±0.011*
		10	633.39±34.37*	270.08±17.70	0.427±0.020*
	OBX/desipramine	10	432.11±33.61*	160.03±18.39	0.370±0.030*
Amygdala	Sham/vehicle	–	444.44±29.09	130.89±9.20	0.294±0.004
	Sham/desipramine	10	425.44±17.29	125.55±11.03	0.298±0.030
	Sham/SNC80	10	424.59±18.01	129.08±9.52	0.299±0.032
	OBX/vehicle	–	226.72±28.98#	90.45±14.34#	0.407±0.046#
		1	535.54±44.56*	178.18±14.82*	0.339±0.028
	OBX/SNC80	3	674.62±48.43*	169.67±15.12*	0.253±0.019
		10	765.00±28.01*	232.88±5.80*	0.306±0.010
	OBX/desipramine	10	460.78±50.20*	170.08±15.45*	0.387±0.041

Data are expressed as means±SEM ($n=7$).
#$P<0.05$ vs. sham-operated rats. *$P<0.05$ vs. vehicle-treated OB rats.

day 7 compared with those on day 1. Thus, it was indicated that SNC80 produced antidepressant-like effects in OBX rats in a time-dependent manner. These are the first results that demonstrate that the abnormal behavior induced by OBX in rats can be counteracted by chronic treatment with the delta-opioid receptor agonist SNC80.

In contrast to this observation, Torregrossa et al. (2005) reported that chronic treatment with a delta-opioid receptor agonist (+)BW373U86 led to the development of tolerance to the antidepressant-like effects in the forced swim test in normal rats. The present study showed that chronic SNC80 treatment did not produce any significant effects in sham rats in terms of not only the emotional scores but also the time spent in the open arm. Thus, it is quite likely that chronic SNC80 treatment led to the development of tolerance in sham-operated rats. The results suggest that abnormal OBX-induced behavior is reversed almost exclusively by chronic but not acute treatment with antidepressants (Song and Leonard, 1994; Cryan et al., 2002). Thus, we suggest that OBX animal models may be useful for predicting the antidepressant action of delta-opioid receptor agonists following chronic administration.

Chronic treatment of OBX rats with the vehicle resulted in minimal weight gain for 8 days. In addition, chronic desipramine treatment in OBX rats resulted in continued weight loss. On the other hand, chronic exposure to SNC80 (3 and 10 mg/kg) did not affect the amount of weight gained by either OBX or sham-operated rats. These results are similar to previous reports in which the chronic administration of (+)BW373U86, a delta-opioid receptor agonist, to rats at a dose of 10 mg/kg did not significantly affect weight gain, while animals that were chronically treated with desipramine lost weight (Torregrossa et al., 2005).

It has been reported that the decreases in tissue 5-HT and 5-HIAA levels were most apparent in the frontal cortex and amygdala of OBX rats (Jancsar and Leonard, 1984; Redmond et al., 1997). On the other hand, a higher level of 5-HT turnover in the hypothalamus was observed in OBX rats (Marcilhac et al., 1999). Similarly, we found that the levels of 5-HT and 5-HIAA in the frontal cortex and in limbic areas such as the hippocampus and amygdala were decreased in OBX rats, while the 5-HT turnover ratio in the hypothalamus was increased. Thus, it appears that our neurochemical data on OBX rats were consistent with those of several reports. Furthermore, subchronic treatment of OBX rats with SNC80 reverses the decrease in the levels of 5-HT and its metabolite 5-HIAA in the frontal cortex, hippocampus, and amygdala

and the increase in the 5-HT level in the hypothalamus. It was also showed that desipramine normalized the levels of 5-HT and 5-HIAA in the amygdala and hypothalamus, as reported previously (Iwasaki et al., 1986). Furthermore, these are the first histological evidence that OBX procedure significantly decreased TH-positive cells in the dorsal

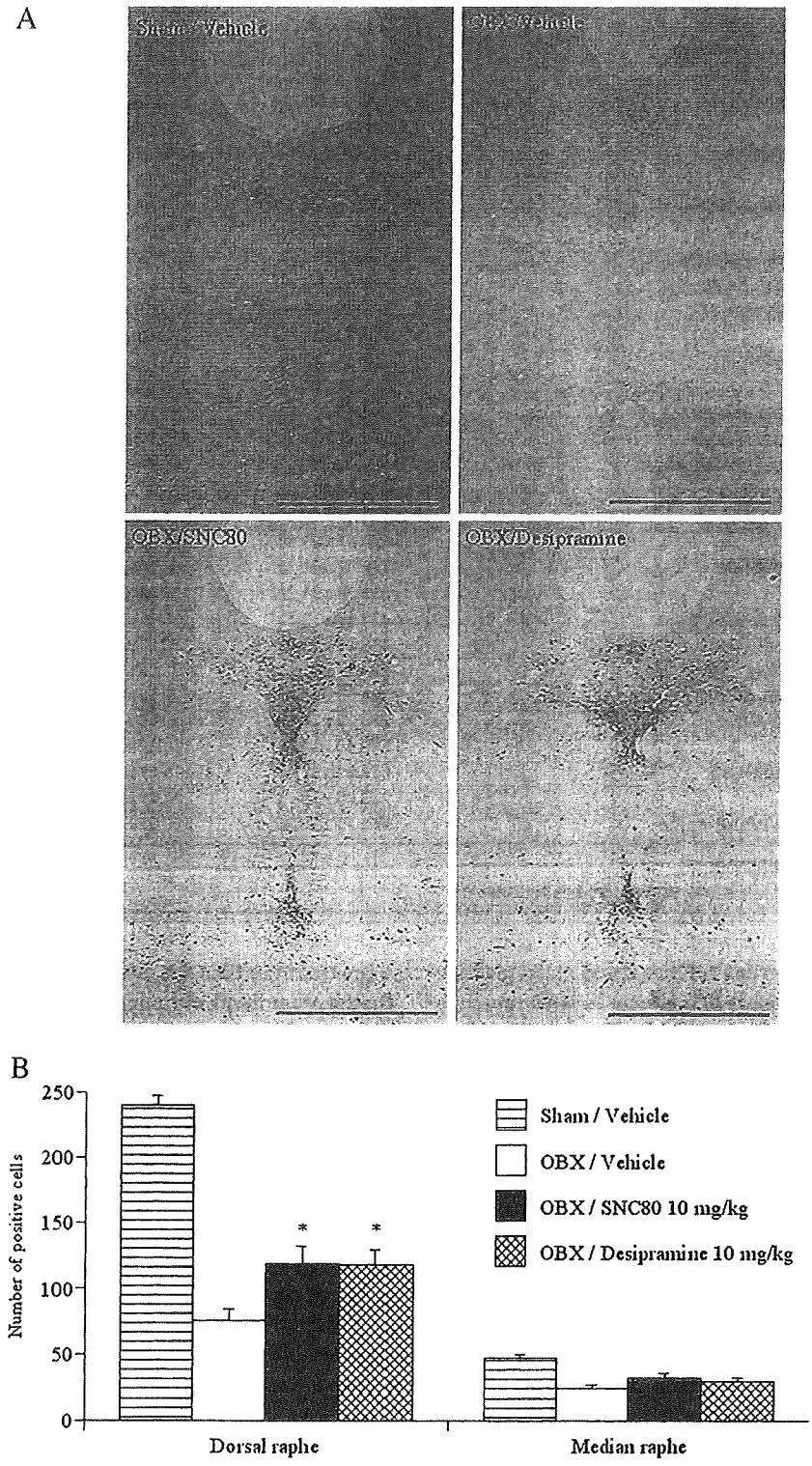

Fig. 4 – Effects of chronic SNC80 treatment on the number of tryptophane hydroxylase (TH)-positive cells in dorsal or median raphe of OBX rats. SNC80 and desipramine were administered chronically once daily for 8 days. TH immunostaining of sections through the dorsal and median raphe prepared from sham- or drug-treated OBX rats (A). Most of the TH-positive cells are located in the dorsal raphe of the midbrain (A). The results are the mean with ±S.E.M. number of TH-positive cells in dorsal or median raphe ($n=8$) (B). Scale bars: 1.0 mm. *$P<0.05$ vs. vehicle-treated OBX rats.

raphe, but not the median raphe, compared with sham-operated rats. Indeed, this result indicated the loss dysfunction of cell bodies on presynaptic serotonergic neurons in the dorsal raphe. These results strongly supported the previous report that abnormalities in the serotonergic system were most apparent in the dorsal raphe of OBX rats (Redmond et al., 1997) and that OBX was decreased the basal extra cellular levels in the basolateral amygdala in microdialysis study (van der Stelt et al., 2005). Indeed, our results demonstrated that SNC80 normalized the OBX-induced serotonergic neuronal changes over a wider area of the brain. It is well known that limbic-cortical areas such as the frontal cortex, hippocampus, hypothalamus, and amygdala that contain the main projections from the dorsal raphe nucleus are important for regulating mood and anxiety/panic. Thus, we propose that the improvement of serotonergic abnormalities in hypothalamus and amygdala observed by chronic SNC80 and/or desipramine treatment may play a key role in improving hyperemotionality and decreasing the time spent and/or entries made in the open arm in OBX rats.

Recently, it was reported that the OBX procedure resulted in a significant reduction of neurogenesis in the hippocampal and subventricular zone and that these deficiencies are normalized by subchronic antidepressant treatment (Jaako-Movits et al., 2006; Keilhoff et al., 2006). On the other hand, it was reported that delta-opioid receptor agonists increase brain-derived neurotrophic factor (BDNF) gene expression across several brain regions (Torregrossa et al., 2004). Furthermore, it was suggested that the stimulation of the delta-opioid receptor may mediate neurogenesis and neuroprotection through BDNF release (Narita et al., 2006). Although further investigation is required, our present findings suggest that improvement of serotonergic abnormalities in the limbic-cortical area by chronic SNC80 treatment may be involved in delta-opioid receptor-induced neurogenesis.

In conclusion, we demonstrated that chronic SNC80 treatment could completely reverse OBX-induced behavioral abnormalities. In addition, we suggest that the improvement of serotonergic abnormalities in the limbic-cortical area that contain the main projections from the raphe nucleus by chronic SNC80 treatment may play a key role in the improvement of hyperemotionality in OBX rats. Finally, we propose that the chronic activity of the delta-opioid receptor might produce potent antidepressant-like effects in an OBX rat model.

4. Experimental procedures

4.1. *Animals*

Seven-week-old male Wistar rats (260–280 g, Tokyo Laboratory Animals Science Co., Ltd., Tokyo, Japan) were used. They had free access to food and water in an animal room that was maintained at 22±1 °C with a 12-h light-dark cycle (lights were automatically put on at 8:00 AM). This study was carried out in accordance with the Declaration of Helsinki and the Guide for the Care and Use of Laboratory Animals of Hoshi University, which is accredited by the Ministry of Education, Science, Sports and Culture.

4.2. *Olfactory bulbectomy-induced hyperemotionality in rats*

Animals were anesthetized with sodium pentobarbital (40 mg/kg i.p.) and placed in a stereotactic apparatus (ASI Instruments, Inc., USA). The olfactory bulbs were removed by suctioning with an aspirator. Postoperatively, the animals were housed in single cages (75.5×21×17 cm) and handled regularly. All animals received gentamycine sulfate antibiotic and ketofen analgesics. At 14 days postsurgery, emotionality was measured using a modification of the OBX-induced hyperemotionality score procedure described by Brady and Nauta (1955) and Shibata et al. (1984). The hyperemotionality of rats was measured by scoring their responses to the following stimuli: (1) attack response was scored by presenting a rod 4–5 cm in front of the snout, (2) startle response was scored by blowing air on the dorsum using a 5-ml syringe, (3) struggle response was scored by handling with a gloved hand, and (4) fight response was scored by pinching the tail with forceps. The rat's tail was gently held from behind using mosquito forceps. A trained researcher performed each of these operations. The responses were graded as follows: 0, no reaction; 1, slight; 2, moderate; 3, marked; or 4, extreme. During each emotional response, vocalization during the test was also scored and graded as follows: 0, no vocalization; 1, occasional vocalization; or 2, marked vocalization. The vocal score was added to each emotional response score. The total emotional response score was the sum of these scores. In each group, all animals were observed on the same day, and each animal was tested within 5 min. The observers were blind with respect to the drug treatment. Only OBX rats that exhibited hyperemotionality (total emotional response score was >14%, 10%, or less of a total postoperated rats) were selected for further study.

4.3. *Elevated plus-maze test*

The plus-maze (Neuroscience, Inc., Tokyo, Japan) consisted of a black plexiglas apparatus with two open arms, 50×10 cm, and two closed arms, 50×10×50 cm, with an open roof; these arms are arranged such that the two open arms are opposite to each other (Pellow et al., 1985). Two opposing arms are delimited by vertical walls (closed arms), whereas the other two opposing arms have unprotected edges (open arms). The maze was elevated 70 cm above the ground and placed in indirect light. At the beginning of the 5-min test session, each rat was placed in the central platform area and faced one of the open arms. Several classical parameters were monitored during the session, including the following: (1) open arm duration, i.e., the total amount of time spent by the rat in an open arm; (2) closed arm duration, i.e., the total amount of time spent by the rat in a closed arm; (3) open arm entries, i.e., the total number of entries with all four paws into the open unprotected arms; (4) closed arm entries, i.e., the total number of entries with all four paws into the closed protected arms; and (5) open arm frequencies, i.e., the ratio of cumulative time spent in the open arms to the total time expressed as a percentage of the time spent in the open arms. The ratio of the cumulative number of visits to the open arms to the total number of visits was expressed as the percentage of open arm entries. The total number of visits and the cumulative time spent were then determined automatically on a monitor through a video camera system. All of the data

were stored in a personal computer and analyzed using analytical software (Comp ACT HBS, Muromachi Kikai, Japan). This protocol was based on that previously described (Saitoh et al., 2003).

4.4. *Analysis of the concentration of 5-HT and its metabolite*

The concentrations of 5-HT and its major metabolite 5-hydroxyindoleacetic acid (5-HIAA) were determined by high-performance liquid chromatography (HPLC). Two hours after the last administration (8th day), the animals performed the elevated plus-maze test. Immediately after the elevated plus-maze tests, all rats were killed by decapitation. The frontal cortex, hippocampus, hypothalamus, and amygdala were quickly dissected and placed on an ice-cold glass plate. These brain tissues were stored at −80 °C until further use. The tissues were homogenized in 300 μl of 0.2 M perchloric acid containing 100 μM EDTA (2 Na) and 100 ng isoproterenol as an internal standard. To remove the proteins completely, the homogenates were placed in cold water for 30 min and then centrifuged at 14,500×*g* for 15 min at 0 °C; the upper layer was maintained at pH 3.0 using 1 M sodium acetate. Solution samples of volume 20 μl were analyzed by HPLC using electrochemical detection. The electrochemical detector (ECD-300, Eicom Co., Kyoto, Japan) was equipped with a graphite electrode (WE-3G, Eicom Co., Kyoto, Japan) that was used at a voltage setting of 750 mV vs. an Ag/AgCl reference electrode. The mobile phase consisted of a 0.1 M sodium acetate/0.1 M citric acid buffer (pH 3.5) containing 17% methanol, 210 mg/l sodium 1-octanesulfonate, and 5 mg/l EDTA (2 Na). The monoamines were separated on a C-18 column (150 mm×3.0 mm reversed-phase, EICOMPAK SC-5ODS, Eicom Co., Kyoto, Japan). The mobile phase flow rate was maintained at 0.5 ml/min with a column temperature of 25 °C.

4.5. *Immunohistochemistry*

To completely fix the time point at which measurement of the effects of SNC80 on the OBX-induced behavioral abnormalities and defects in serotonergic function, we prepared the different set of rats for the behavioral study, measurement of serotonin concentration and TH-positive cells counts. Two hours after the last administration (8th day), animals were anaesthetized with pentobarbital (130 mg/kg; Sigma, St. Quentin, France) and transcardially perfused with 4% paraformaldehyde in 0.1 M phosphate buffer (PB) after the elevated plus-maze tests. Brains were removed, postfixed, and cryoprotected. Immunohistochemistry was performed on free-floating cryomicrotome-cut sections (20 μm thick) encompassing the entire dorsal raphe and median raphe. After incubation in 3% H_2O_2/20% methanol, followed by 0.2% Triton X-100 and 2% w/v bovine serum albumin in 0.1M PBS, the sections were stained overnight at 4 °C using a polyclonal antibody against tryptophane hydroxylase (1:1000; Pel Freez, Rogers, AR, USA) for serotonergic neurons. Sections were then treated with secondary antibodies (Vectastain; Vector Laboratory, Burlingame, CA, USA), and subsequently incubated with avidin-biotinylated horseradish peroxidase complex. The peroxidase was revealed by incubation with 0.05% 3,3'-diaminobenzidine tetrahydrochloride containing 0.015% hydrogen peroxide. For Nissl cell counts, TH sections were counterstained with cresyl violet. All sections for a given marker were stained simultaneously for all animals using the same solutions.

4.6. *Data analysis*

The data are expressed as means ± S.E.M. The statistical significance of the differences in the behavioral data between two groups was assessed by two-way analysis of variance (ANOVA), and post hoc individual group comparisons were made by the Tukey–Kramer test. Analyses were performed using the StatView statistical software (SAS Institute Inc., Cary, NC, USA). P-values less than 0.05 were considered significant.

4.7. *Drugs*

The drugs used in the present study were desipramine (Sigma Chemical Co., St. Louis, MO, USA) and (+)-4-[(aR)-a-((2S,5R)-4-allyl-2,5-dimethyl-1-piperazinyl)-3-methoxybenzyl]-*N*, *N*-diethylbenzamide tartaric acid (SNC80) (synthesized by Toray Industries, Inc.). Both drugs were dissolved in physiological saline. Each drug was injected i.p. in a volume of 1 ml/kg body weight. For chronic administration, SNC80, desipramine, or vehicle was administered i.p. once daily for a total of 8 days. On day 7 after the 14-day postsurgical period, the emotional responses were measured 120 min after drug administration. On day 8, OBX rats received drugs 120 min before the elevated plus-maze test.

Acknowledgments

We would like to thank Drs. K. Kawai, T. Suzuki, and K. Hasebe (Toray Industries, Inc.) for their constant support.

REFERENCES

Baamonde, A., Dauge, V., Ruiz-Gayo, M., Fulga, I.G., Turcaud, S., Fournie-Zaluski, M.C., Roques, B.P., 1992. Antidepressant-type effects of endogenous enkephalins protected by systemic RB 101 are mediated by opioid delta and dopamine D1 receptor stimulation. Eur. J. Pharmacol. 216, 157–166.

Brady, J.V., Nauta, W.J., 1955. Subcortical mechanisms in emotional behavior: the duration of affective changes following septal and habenular lesions in the albino rat. J. Comp. Physiol. Psychol. 48, 412–420.

Broom, D.C., Jutkiewicz, E.M., Folk, J.E., Traynor, J.R., Rice, K.C., Woods, J.H., 2002. Nonpeptidic delta-opioid receptor agonists reduce immobility in the forced swim assay in rats. Neuropsychopharmacology 26, 744–755.

Chaki, S., Nakazato, A., Kennis, L., Nakamura, M., Mackie, C., Sugiura, M., Vinken, P., Ashton, D., Langlois, X., Steckler, T., 2004. Anxiolytic- and antidepressant-like profile of a new CRF1 receptor antagonist, R278995/CRA0450. Eur. J. Pharmacol. 485, 145–158.

Cryan, J.F., Markou, A., Lucki, I., 2002. Assessing antidepressant activity in rodents: recent developments and future needs. Trends Pharmacol. Sci. 23, 238–245.

Filliol, D., Ghozland, S., Chluba, J., Martin, M., Matthes, H.W., Simonin, F., Befort, K., Gaveriaux-Ruff, C., Dierich, A., LeMeur,

M., Valverde, O., Maldonado, R., Kieffer, B.L., 2000. Mice deficient for delta- and mu-opioid receptors exhibit opposing alterations of emotional responses. Nat. Genet. 25, 195–200.

Ho, Y., Liu, T., Tai, M., Wen, Z., Chow, R.S., Tsai, Y., Wong, C., 2001. Effects of olfactory bulbectomy on NMDA receptor density in the rat brain. Brain Res. 900, 214–218.

Hasegawa, S., Watanabe, A., Nguyen, K.Q., Debonnel, G., Diksic, M., 2005. Chronic administration of citalopram in olfactory bulbectomy rats restores brain 5-HT synthesis rates: an autoradiographic study. Psychopharmacology (Berl). 179, 781–790.

Ho, Y.J., Chen, K.H., Tai, M.Y., Tsai, Y.F., 2004. MK-801 suppresses muricidal behavior but not locomotion in olfactory bulbectomized rats: involvement of NMDA receptors. Pharmacol. Biochem. Behav. 77, 641–646.

Iwasaki, K., Fujiwara, M., Shibata, S., Ueki, S., 1986. Changes in brain catecholamine levels following olfactory bulbectomy and the effect of acute and chronic administration of desipramine in rats. Pharmacol. Biochem. Behav. 24, 1715–1719.

Jaako-Movits, K., Zharkovsky, T., Pedersen, M., Zharkovsky, A., 2006. Decreased hippocampal neurogenesis following olfactory bulbectomy is reversed by repeated citalopram administration. Cell. Mol. Neurobiol. 26, 1559–1570.

Jancsar, S.M., Leonard, B.E., 1984. Changes in neurotransmitter metabolism following olfactory bulbectomy in the rat. Prog. Neuropsychopharmacol. Biol. Psychiatry 8, 263–269.

Jutkiewicz, E.M., Eller, E.B., Folk, J.E., Rice, K.C., Traynor, J.R., Woods, J.H., 2004. Delta-opioid agonists: differential efficacy and potency of SNC80, its 3-OH (SNC86) and 3-desoxy (SNC162) derivatives in Sprague–Dawley rats. J. Pharmacol. Exp. Ther. 309, 173–181.

Jutkiewicz, E.M., Rice, K.C., Traynor, J.R., Woods, J.H., 2005a. Separation of the convulsions and antidepressant-like effects produced by the delta-opioid agonist SNC80 in rats. Psychopharmacology 182, 588–596.

Jutkiewicz, E.M., Kaminsky, S.T., Rice, K.C., Traynor, J.R., Woods, J.H., 2005b. Differential behavioral tolerance to the δ-opioid agonist SNC80 ((+)-4-[(αR)-α-[(2S,5R)-2, 5-dimethyl-4-(2-propenyl)-1-piperazinyl]-(3-methoxyphenyl) methyl]-N,N-diethylbenzamide) in Sprague–Dawley rats. J. Pharmacol. Exp. Ther. 315, 414–422.

Keilhoff, G., Becker, A., Grecksch, G., Bernstein, H.G., Wolf, G., 2006. Cell proliferation is influenced by bulbectomy and normalized by imipramine treatment in a region-specific manner. Neuropsychopharmacology 31, 1165–1176.

Kelly, J.P., Wrynn, A.S., Leonard, B.E., 1997. The olfactory bulbectomized rat as a model of depression: an update. Pharmacol. Ther. 74, 299–316.

Konig, M., Zimmer, A.M., Steiner, H., Holmes, P.V., Crawley, J.N., Brownstein, M.J., Zimmer, A., 1996. Pain responses, anxiety and aggression in mice deficient in pre-proenkephalin. Nature 383, 535–538.

Lumia, A.R., Teicher, M.H., Salchli, F., Ayers, E., Possidente, B., 1992. Olfactory bulbectomy as a model for agitated hyposerotonergic depression. Brain Res. 587, 181–185.

Marcilhac, A., Faudon, M., Anglade, G., Hery, F., Siaud, P., 1999. An investigation of serotonergic involvement in the regulation of ACTH and corticosterone in the olfactory bulbectomized rat. Pharmacol. Biochem. Behav. 63, 599–605.

Narita, M., Kuzumaki, N., Miyatake, M., Sato, F., Wachi, H., Seyama, Y., Suzuki, T., 2006. Role of delta-opioid receptor function in neurogenesis and neuroprotection. J. Neurochem. 97, 1494–1505.

Okuyama, S., Chaki, S., Kawashima, N., Suzuki, Y., Ogawa, S., Nakazato, A., Kumagai, T., Okubo, T., Tomisawa, K., 1999. Receptor binding, behavioral, and electrophysiological profiles of nonpeptide corticotropin-releasing factor subtype 1 receptor antagonists CRA1000 and CRA1001. J. Pharmacol. Exp. Ther. 289, 926–935.

Pellow, S., Chopin, P., File, S.E., Briley, M., 1985. Validation of open: closed arm entries in an elevated plus-maze as a measure of anxiety in the rat. J. Neurosci. Methods 14, 149–167.

Perrine, S.A., Hoshaw, B.A., Unterwald, E.M., 2006. Delta opioid receptor ligands modulate anxiety-like behaviors in the rat. Br. J. Pharmacol. 147, 864–872.

Ragnauth, A., Schuller, A., Morgan, M., Chan, J., Ogawa, S., Pintar, J., Bodnar, R.J., Pfaff, D.W., 2001. Female preproenkephalin-knockout mice display altered emotional responses. Proc. Natl. Acad. Sci. 98, 1958–1963.

Redmond, A.M., Kelly, J.P., Leonard, B.E., 1997. Behavioural and neurochemical effects of dizocilpine in the olfactory bulbectomized rat model of depression. Pharmacol. Biochem. Behav. 58, 355–359.

Saitoh, A., Yamaguchi, K., Murasawa, H., Kamei, J., 2003. The approaches in the discovery of antidepressants using affective disorder models. Jpn. J. Neuropsychopharmacology 23, 75–82.

Saitoh, A., Kimura, Y., Suzuki, T., Kawai, K., Nagase, H., Kamei, J., 2004. Potential anxiolytic and antidepressant-like activities of SNC80, a selective delta-opioid agonist, in behavioral models in rodents. J. Pharmacol. Sci. 95, 374–380.

Saitoh, A., Yoshikawa, Y., Onodera, K., Kamei, J., 2005. Role of delta-opioid receptor subtypes in anxiety-related behaviors in the elevated plus-maze in rats. Psychopharmacology 182, 327–334.

Saitoh, A., Hirose, N., Yamada, M., Yamada, M., Nozaki, C., Oka, T., Kamei, J., 2006. Changes in emotional behavior of mice in the hole-board test after olfactory bulbectomy. J Pharmacol. Sci. 102, 377–386.

Saitoh, A., Yamaguchi, K., Tatsumi, Y., Murasawa, H., Nakatani, A., Hirose, N., Yamada, M., Yamada, M., Kamei, J., 2007. Effects of milnacipran and fluvoxamine on hyperemotional behaviors and the loss of tryptophan hydroxylase-positive cells in olfactory bulbectomized rats. Psychopharmacology (Berl) 191, 857–865.

Shibata, S., Nakanishi, H., Watanabe, S., Ueki, S., 1984. Effects of chronic administration of antidepressants on mouse-killing behavior (muricide) in olfactory bulbectomized rats. Pharmacol. Biochem. Behav. 21, 225–230.

Song, C., Leonard, B.E., 1994. Serotonin reuptake inhibitors reverse the impairments in behaviour neurotransmitter and immune functions in the olfactory bulbectomized rat. Hum. Psychopharmacol. 9, 135–146.

Song, C., Leonard, B.E., 2005. The olfactory bulbectomised rat as a model of depression. Neurosci. Biobehav. Rev. 29, 627–647.

Tejedor-Real, P., Mico, J.A., Smadja, C., Maldonado, R., Roques, B.P., Gilbert-Rahola, J., 1998. Involvement of delta-opioid receptors in the effects induced by endogenous enkephalins on learned helplessness model. Eur. J. Pharmacol. 354, 1–7.

Thorne, B.M., Rowles, J.S., 1988. Memory deficit in passive-avoidance learning in bulbectomized Long–Evans hooded rats. Physiol. Behav. 44, 339–345.

Torregrossa, M.M., Isgor, C., Folk, J.E., Rice, K.C., Watson, S.J., Woods, J.H., 2004. The delta-opioid receptor agonist (+) BW373U86 regulates BDNF mRNA expression in rats. Neuropsychopharmacology 29, 649–659.

Torregrossa, M.M., Folk, J.E., Rice, K.C., Watson, S.J., Woods, J.H., 2005. Chronic administration of the delta opioid receptor agonist (+)BW373U86 and antidepressants on behavior in the forced swim test and BDNF mRNA expression in rats. Psychopharmacology 183, 31–40.

Torregrossa, M.M., Jutkiewicz, E.M., Mosberg, H.I., Balboni, G., Watson, S.J., Woods, J.H., 2006. Peptidic delta opioid receptor agonists produce antidepressant-like effects in the forced swim test and regulate BDNF mRNA expression in rats. Brain Res. 1069, 172–181.

van der Stelt, H.M., Breuer, M.E., Olivier, B., Westenberg, H.G., 2005. Permanent deficits in serotonergic functioning of olfactory bulbectomized rats: an in vivo microdialysis study. Biol. Psychiatry. 1, 1061–1067.

Watanabe, A., Tohyama, Y., Nguyen, K.Q., Hasegawa, S., Debonnel, G., Diksic, M., 2003. Regional brain serotonin synthesis is increased in the olfactory bulbectomy rat model of depression: an autoradiographic study. J. Neurochem. 85, 469–475.

Yamaguchi, K., Murasawa, H., Kyuki, K., 2002. Animal models to elucidate depression and anxiety: usability of hyperemotionality and time on closed-arms of an elevated plus-maze (+maze) in olfactory bulbectomized (OB) rats. Jpn. J. Pharmacol. 88, 235.

Zhou, D., Grecksch, G., Becker, A., Frank, C., Pilz, J., Huether, G., 1998. Serotonergic hyperinnervation of the frontal cortex in an animal model of depression, the bulbectomized rat. J. Neurosci. Res. 54, 109–116.

ORIGINAL ARTICLE

Genome-Wide Association for Methamphetamine Dependence

Convergent Results From 2 Samples

George R. Uhl, MD, PhD; Tomas Drgon, PhD; Qing-Rong Liu, PhD; Catherine Johnson, MSc; Donna Walther, MSc; Tokutaro Komiyama, MD; Mutsuo Harano, MD; Yoshimoto Sekine, MD, PhD; Toshiya Inada, MD; Norio Ozaki, MD, PhD; Masaomi Iyo, MD, PhD; Nakao Iwata, MD, PhD; Mitsuhiko Yamada, MD; Ichiro Sora, MD, PhD; Chih-Ken Chen, MD, PhD; Hsing-Cheng Liu, MD, PhD; Hiroshi Ujike; Shih-Ku Lin, MD

Context: We can improve understanding of human methamphetamine dependence, and possibly our abilities to prevent and treat this devastating disorder, by identifying genes whose allelic variants predispose to methamphetamine dependence.

Objective: To find "methamphetamine dependence" genes identified by each of 2 genome-wide association (GWA) studies of independent samples of methamphetamine-dependent individuals and matched controls.

Design: Replicated GWA results in each of 2 case-control studies.

Setting: Japan and Taiwan.

Participants: Individuals with methamphetamine dependence and matched control subjects free from psychiatric, substance abuse, or substance dependence diagnoses (N=580).

Main Outcome Measures: "Methamphetamine dependence" genes that were reproducibly identified by clusters of nominally positive single-nucleotide polymorphisms (SNPs) in both samples in ways that were unlikely to represent chance observations, based on Monte Carlo simulations that corrected for multiple comparisons, and subsets of "methamphetamine dependence" genes that were also identified by GWA studies of dependence on other addictive substances, success in quitting smoking, and memory.

Results: Genes identified by clustered nominally positive SNPs from both samples were unlikely to represent chance observations (Monte Carlo $P<.00001$). Variants in these "methamphetamine dependence" genes are likely to alter cell adhesion, enzymatic functions, transcription, cell structure, and DNA, RNA, and/or protein handling or modification. Cell adhesion genes *CSMD1* and *CDH13* displayed the largest numbers of clustered nominally positive SNPs. "Methamphetamine dependence" genes overlapped, to extents much greater than chance, with genes identified in GWA studies of dependence on other addictive substances, success in quitting smoking, and memory (Monte Carlo P range $<.04$ to $<.00001$).

Conclusion: These data support polygenic contributions to methamphetamine dependence from genes that include those whose variants contribute to dependence on several addictive substances, success in quitting smoking, and mnemonic processes.

Arch Gen Psychiatry. 2008;65(3):345-355

METHAMPHETAMINE abuse is a growing problem in many regions of the United States and a long-standing concern in Taiwan and Japan. Elucidating which genetic variants enhance individuals' vulnerability should increase our understanding of methamphetamine dependence.

Recent reviews suggest that addictive substance dependence is likely to display a polygenic genetic architecture.[1,2] Psychostimulant dependence displays strong familial and genetic influences in family and twin studies.[3-18] Individual differences in vulnerability to methamphetamine are thus likely to display substantial genetic determinants. Since much of the genetic vulnerability to stimulant abuse overlaps with the genetics of vulnerability to other classes of addictive substances, it is likely that methamphetamine dependence displays such genetic overlaps as well.[13-16,19] However, there is no evidence that any single gene's variants mediate a large portion of vulnerability to psychostimulant dependence.

Identifying the genes that harbor allelic variants that contribute to human individual differences in vulnerabilities to methamphetamine dependence will help us to understand processes that underlie human addictions. We may improve understanding of the relative contributions of variants in the brain systems that underlie

Author Affiliations are listed at the end of this article.

Downloaded from www.archgenpsychiatry.com at Nenp, on December 4, 2008
©2008 American Medical Association. All rights reserved.